Published in final edited form as:
Dev Biol. 2007 April 1; 304(1): 338–354.

Redundant activities of Tfap2a and Tfap2c are required for neural crest induction and development of other non-neural ectoderm derivatives in zebrafish embryos

Wei Li[1] and **Robert Cornell**[1,2]

1 *Interdisciplinary Graduate Program in Genetics, Carver College of Medicine, University of Iowa, Iowa City, Iowa, 52242*

2 *Department of Anatomy and Cell Biology, Carver College of Medicine, University of Iowa, Iowa City, Iowa, 52242*

Abstract

Knockdown studies suggest transcription factor AP-2 alpha (Tfap2a), is required for neural crest induction in frog embryos. Because *tfap2a* is expressed in neural crest and in presumptive epidermis, a source of signals that induce neural crest, it was unclear whether this requirement was cell autonomous. Moreover, neural crest induction occurs normally in zebrafish *tfap2a* and mouse *Tcfap2a* mutant embryos, so it was unclear if a requirement for Tfap2a in this process was evolutionarily conserved. Here we show that zebrafish *tfap2c*, encoding AP-2 gamma (Tfap2c), is expressed in non-neural ectoderm including transiently in neural crest. Inhibition of *tfap2c* with antisense oligonucleotides does not visibly perturb development. However, simultaneous inhibition of *tfap2a* and *tfap2c* utterly prevents neural crest induction, and disrupts development of cranial placode derivatives, although gene expression characteristic of the pre-placodal domain is normal. Transplant studies support a cell-autonomous role for Tfap2a and Tfap2c in neural crest induction. Unexpectedly, Rohon-Beard sensory neurons, which previous studies indicate are derived from the same precursor population as neural crest, are reduced by less than half in *tfap2a/tfap2c* doubly deficient embryos, implying non-neural crest origin for a subset of them. These results reveal a requirement for Tfap2-type activity for early development of all non-neural ectoderm derivatives.

Introduction

The neural crest is a population of precursor cells that migrate from the dorsal neural tube and give rise to diverse derivatives. Neural crest induction refers to the specification of ectoderm cells to the neural crest lineage. This process is of particular interest because it reflects events in the emergence of neural crest during vertebrate evolution. It is believed that combinatorial activity of transcription factors expressed at the neural plate border governs neural crest induction, but the functions of specific transcription factors in this process are not yet clear (Hong and Saint-Jeannet, 2005;Sauka-Spengler and Bronner-Fraser, 2006;Steventon et al., 2005).

The Tfap2 (AP-2 or Activator Protein 2) family of transcription factors is implicated in control of cell induction, differentiation, survival, and proliferation in various developmental contexts, including the neural crest (reviewed in Eckert et al., 2005;Hilger-Eversheim et al., 2000). In

mouse, the five Tfap2 proteins, a–e, are encoded by the genes *Tcfap2a*, *Tcfap2b*, etc., respectively; in humans and frogs the orthologues of these genes are *TFAP2A*, etc., and in zebrafish, they are known as *tfap2a*, etc. The five proteins share a conserved structure, and with the exception of Tfap2d, they share very similar DNA binding specificity (Eckert et al., 2005). Mutant analysis has shown that Tfap2a is essential for normal development of neural crest derivatives (Holzschuh et al., 2003;Knight et al., 2004;Schorle et al., 1996;Zhang et al., 1996). However the role of Tfap2a specifically in neural crest induction has remained uncertain, because disruption of Tfap2a expression has different effects in different species. Oligonucleotide-mediated knock down of *TFAP2A* in frog embryos greatly, but not completely, reduced expression of *Slug* and *Sox9*, two markers of pre-migratory neural crest, and forced expression of *TFAP2A* in neural plate or in explanted, neuralized ectoderm induced ectopic expression of these genes (Luo et al., 2003;Luo et al., 2005). These experiments suggested that Tfap2a is required for specification of neural crest in frogs, in a cell autonomous or non-autonomous mode. By contrast, in mouse and zebrafish *Tcfap2a* (*tfap2a*) strong hypomorphic or null mutants induction and migration of neural crest appear to occur essentially normally (Barrallo-Gimeno et al., 2004;Knight et al., 2003;Schorle et al., 1996;Zhang et al., 1996). These disparities suggested the possibility that a role for Tfap2-type activity in neural crest induction might not be a conserved feature among vertebrates.

Alternatively, there may be variation among species in the degree to which neural crest induction is shared among Tfap2 family members. *Tcfap2a*, *Tcfap2b*, and *Tcfap2c* are all expressed in neural crest in mouse (Chazaud et al., 1996;Mitchell et al., 1991;Moser et al., 1997), and there is evidence that Tfap2 family members act redundantly in development. For instance, *Tcfap2a* and *Tcfap2c* are co-expressed in extra-embryonic tissue (Auman et al., 2002;Werling and Schorle, 2002;Winger et al., 2006). Mouse *Tcfap2c* mutants die at 8.5 days post coitum (dpc) because of abnormal placental function (Auman et al., 2002;Werling and Schorle, 2002). By contrast, mouse *Tcfap2a* mutant embryos live considerably longer, until shortly after birth (Schorle et al., 1996;Zhang et al., 1996). Embryos doubly mutant for *Tcfap2a* and *Tcfap2c* die at 3.5 dpc, i.e., even earlier than *Tcfap2c* mutants, consistent with redundant activity of these proteins within extra embryonic tissue during mouse peri-implantation development (Winger et al., 2006). In another example, zebrafish *tfap2b* is expressed in the hindbrain and, like *tfap2a*, in non-neural ectoderm flanking the hindbrain (Knight et al 2005). Oligonucleotide-mediated knockdown of *tfap2b* did not visibly perturb development, but simultaneous inhibition of *tfap2a* and *tfap2b* resulted in far more severe defects in craniofacial cartilage than in *tfap2a* mutants, apparently because of redundant activity of Tfap2a and Tfap2b in cranial epidermis (Knight et al 2005). Because Tfap2 family members appear to act redundantly in other developmental contexts they may do so during neural crest induction.

A second open question regarding the role of Tfap2-type activity in neural crest induction is whether this role is direct or indirect. In mice and zebrafish, *Tcfap2a/tfap2a* is expressed from gastrula stages in premigratory neural crest, but also in non-neural ectoderm flanking the neural crest. Explant studies have shown that non-neural ectoderm is the source of signals that induce neural crest (Dickinson et al., 1995;Liem et al., 1995;Moury and Jacobson, 1990;Selleck and Bronner-Fraser, 1995), so it is possible the production of these signals depends on Tfap2-type activity. Consistent with this possibility, there is evidence that signals from adjacent tissues that instill pattern on neural crest cells depend on Tfap2-type activity. Thus, in mouse *Tcfap2a* mutant embryos and zebrafish *tfap2a* mutant embryos, there is a profound reduction in a subset of neural crest derivatives including the jaw (Barrallo-Gimeno et al., 2004;Holzschuh et al., 2003;Knight et al., 2003;Schorle et al., 1996;Zhang et al., 1996). However, this dependence of jaw development on Tfap2a is at least partially cell non-autonomous, because embryos with Wnt1-Cre mediated neural crest-specific elimination of *Tcfap2a* have normal jaws (Brewer et al., 2004), and the presence of wild-type pharyngeal

ectoderm can partially rescue the development of the jaw in zebrafish *tfap2a* mutants (Knight et al., 2005). These examples illustrate that non-autonomous effects of Tfap2-type activity on neural crest development are possible.

Here we address both of these issues in zebrafish embryos. We present evidence that redundant activity of Tfap2a and Tfap2c is required for neural crest induction, and that this requirement is cell autonomous. Unexpectedly, Rohon-Beard spinal sensory neurons, which share properties with neural crest (Artinger, et al. 1999;Cornell and Eisen, 2000;Cornell and Eisen, 2002), are merely reduced in embryos deficient in Tfap2a and Tfap2c. These findings suggest that Tfap2-type activity, mediated by Tfap2a and Tfap2c, is a conserved, and cell-autonomous requirement of neural crest induction. We also describe severe reduction of cranial placode derivatives, but no evidence of a failure of induction of the preplacodal domain, in embryos deficient in both genes.

Materials and Methods

Fish maintenance

Zebrafish embryos and adults were reared as described (Westerfield, 1993) in the University of Iowa Zebrafish Facility. Embryos were staged by hours or days post fertilization at 28.5°C (hpf or dpf) (Kimmel et al., 1995). To generate *tfap2a* homozygous mutant embryos, heterozygous adults harboring a presumed null allele of *tfap2a* (*lockjaw*,Knight et al., 2003) were used.

Identify zebrafish Tfap2 orthologes

Three putative genes encoding zebrafish Tfap2 orthologues were found in the database of the Zebrafish Information Network (ZFIN, http://zfin.org). Genbank accession numbers for these genes are listed: *tfap2c*, NM_001008576; *tfap2d*, NM_00102554; *tfap2e*, NM_200821.

RT-PCR and morpholinos

First-strand cDNA was synthesized from total RNA harvested from embryos at 24 hpf as described (O'Brien et al., 2004). A 1.3 kb fragment of zebrafish *tfap2c* was amplified from the wild-type cDNA by using the following primers: forward, 5′-GTT AGC AGC AAT GGG AAC CCT C-3′, reverse, 5′-GGT ACC ATC GGA AGA GGC TTG T-3′, and inserted into pCR4-TOPO vector (Invitrogen, Carlsbad, CA). This fragment includes most of the open reading frame (i.e., encoding amino acids 22 to 434 of 445).

To disrupt *tfap2c* expression, the exon 3 splice donor site and the exon 4 splice acceptor site were inferred in zebrafish *tfap2c* gene by comparison of cDNA sequence to *tfap2c* genomic sequence (www.ensembl.org/Danio_rerio/index.html, zgc92088). Morpholinos complementary to these sites were ordered: *tfap2c e3i3* MO, 5′-TCT GAC ATC AAC TCA CCT GAA CATC-3′; *tfap2c i3e4* MO, 5′-CAT CGT GCT GCA ATA AAA CAA AAT G-3′ (Gene Tools, Philomath, OR). For a negative control, the vendor's standard control morpholino (5′-CCT CTT ACC TCA GTT ACA ATT TAT A-3′), which is thought to have no specific target in animal cells, was used. Morpholinos were reconstituted to 5 mg/ml in Danieau solution (Nasevicius and Ekker, 2000) and stored at −20°C, then diluted immediately before use to 1 mg/ml in 0.2 M KCl. Embryos were injected with 4–8 nl of diluted morpholinos at the 1–4 cell stage into the yolk immediately below the blastomeres. We saw evidence of non-specific toxicity, i.e., patches of opacity in the brain and spinal cord, upon injection of 10 ng or more of either MO. However, injection of 5 ng of either *tfap2c* MO did not cause this phenotype. We compared efficiency of the MO, and found that 2.5 ng/embryo of *tfap2c e3i3* MO was virtually always sufficient to eliminate melanophores in *tfap2a* homozygous mutants, while 5.0 ng/embryo of *tfap2c i3e4* MO was necessary for this effect. To assure strong penetrance,

5 ng/embryo of *tfap2c e3i3* MO was used to generate *tfap2a*$^{-}$/*c*^{MO} embryos. For double MO experiments, 5 ng of *tfap2c e3i3* MO and 2.5 ng *tfap2a e2i2* MO were injected. *ngn1* MO (Cornell and Eisen, 2002), was used at 1.5 ng/embryo. To test the efficacy of those *tfap2c* MOs, a pair of primers flanking a 557 bp fragment between the exon 3 and exon 5 of *tfap2c* was used for RT-PCR (forward, 5′-AAC CCA GCG ACC CAT ACT CTC A-3′; reverse, 5′-TCC AAG CAG GGA TGC GTT CA-3′).

Chimeric embryo procedure

To create genetic chimeras, donor embryos were injected with 5 nl of 1% lysine-fixable biotinylated-dextran, 10,000 MW (Sigma, St. Louis, MO). At sphere stage (4 hpf), about 100 cells were withdrawn from each donor embryo with a manual-drive syringe fitted with an oil-filled needle (Fine Science Tools, Vancouver, BC), and about 20 cells were inserted into each of several host embryos at the same stage, aiming for a position close to the animal pole, to target clones to ectoderm (Kimmel et al., 1990). Host embryos were allowed to develop to 12 hpf, fixed and processed to reveal *foxd3* gene expression by whole mount in situ hybridization and to reveal biotin with an ABC kit (Vector Labs, Burlingame, CA) and DAB as previously described (Moens and Fritz, 1999). Some host embryos were allowed to develop to 48 hpf, fixed and processed to reveal biotin.

Misexpression and rescue experiments

For rescue experiments, the open reading frame of zebrafish *tfap2a*, isoform AF457191, was amplified from cDNA prepared from 24 hpf embryos using the following primers: forward, 5′-GCA GGA TCC ATG AAA ATG CTT TGG A-3′, with BamHI restriction site added to the 5′ end; reverse, 5′-TAG TTC TAG ATT GGA TAT CAC TTT CTG-3′, with XbaI restriction site added to the 5′ end. The PCR product was ligated into pCS2^{+} vector, creating *pCS2-tfap2a-ORF*. This construct was linearized with NotI and capped *tfap2a* mRNA was generated in vitro with the mMessage mMachine kit (Ambion, Austin, TX). For rescue experiments, *tfap2a* mRNA was injected at a final dose of 0.25–0.5 ng, mixed with *tfap2a* MO and *tfap2c* MO prior to injection. For ectopic expression experiments, capped mRNA was synthesized in vitro from the *GRXAP2* plasmid (Luo et al., 2002) and injected at 0.6–0.8 ng in 0.2 M KCl. *lacz* RNA was synthesized as described (Cornell and Eisen, 2000) and used as a lineage tracer.

Gene expression analysis

DIG-labeled antisense RNA probes (Roche Diagnostics, Mannheim, Germany) used for whole mount in situ hybridization were generated as described previously: *tfap2a*, *msxb*, *foxd3*, *sox10*, *dlx2* (Monsoro-Burq et al., 2005;O'Brien et al., 2004), *isl1* (Cornell and Eisen, 2002), *pax3* (Lewis et al., 2004), *zic2b* (Kudoh et al., 2004), *sox2* (Thisse et al., 2001), *prdm1* (Hernandez-Lagunas et al., 2005); or as follows: *tfap2c*, NotI/T3; *sox9b* (Yan et al., 2005), StuI/T7; *snai1b* (Thisse et al., 1995), XbaI/T7; *dlx3b* (Akimenko et al., 1994), SalI/T7; *eya1* (Sahly et al., 1999), NotI/T7; and *tlxA* (Andermann and Weinberg, 2001), BamHI/T7. Two-color in situ hybridization analysis, using DIG-labeled *tfap2c* probe and FITC-labeled *foxd3* probe, was carried out as described (O'Brien et al., 2004).

Markers of cranial ganglia, enteric neurons, sympathetic neurons, and dorsal root ganglia, including anti-HNK1 (Zn12) (Trevarrow, et al. 1990) and anti-Hu (Marusich, et al. 1994), were used in whole mount immunohistochemistry as described (O'Brien et al., 2004). Double labeling with monoclonal antibody mAb 39.4D5 (anti-Islet proteins) and DIG-labeled *foxd3*/*tfap2a* probes were performed as described (Cornell and Eisen, 2000). Alcian green was used to label pharyngeal cartilage as described (Kimmel et al., 1998).

Apoptosis, cell proliferation, and DASPEI assays

Apoptotic cell death was monitored in whole embryos by terminal transferase dUTP nick-end labeling essentially as described (Reyes et al., 2004), except dUTP-DIG was used. The terminal transferase reaction was stopped by incubation at 70°C for 30 minutes, and embryos were processed with anti-DIG-alkaline phosphatase antibody and developed with NBT/BCIP, as for an RNA in situ hybridization. zVAD-fmk (MP Biomedicals, Irvine, CA) was diluted in fish water to 300 μM and added to the embryos at 6 hpf. To measure proliferation, live embryos at 10 hpf were incubated for 20 minutes in 10 mM bromodeoxyuridine (BrdU) (Roche Diagnostics Mannheim, Germany) in fish water with 15% DMSO at 4°C. Embryos were then rinsed in fish water and allowed to develop till 11 hpf. Anti-bromodeoxyuridine mouse monoclonal antibody (BMC 9318) (Roche Diagnostics, Indianapolis, IN) was used at 1:100 dilution, and developed with the PAP system (Abcam, Cambridge, MA) and DAB. To label hair cells, live embryos were incubated in 1 mM DASPEI (2-(4-dimethylaminostyryl)-N-ethylpyridinium iodide) (Biotium, Hayward, CA) for 60 minutes, rinsed for 30 minutes in embryo medium (Westerfield, 1993), and viewed with epifluorescence optics.

Results

A zebrafish *tfap2c* orthologue is expressed in non-neural ectoderm starting during gastrula stages

We looked for Tfap2 family members that were expressed at the appropriate place and time to participate in neural crest induction, i.e., in lateral ectoderm during gastrula stage. Orthologues of *Tcfap2c*, *Tcfap2d*, and *Tcfap2e* in zebrafish genomic DNA have been identified by sequence comparison algorithms (www.ensembl.org/Danio_rerio). With RT-PCR we amplified partial clones of at least 1 kb from each orthologue, and examined expression of each *in situ* in embryos ranging from 6 hpf (gastrula) to 48 hpf. Expression of neither *tfap2d* nor *tfap2e* is detected in non-neural ectoderm during gastrula stages, so these orthologues were not pursued in the context of neural crest induction (WL and RAC, unpublished data). At 4-cell stage, maternal *tfap2c* transcripts are detected by RT-PCR (not shown). At 6 hpf, *tfap2c* expression is detected in non-neural ectoderm (Fig. 1A), in a pattern similar or identical to that of *tfap2a* (Fig. 1B). At 8.5 hpf, *tfap2c* expression is found to at least partially overlap that of *pax3*, a marker of prospective neural crest (Lewis et al., 2004) (Fig. 1C,D). By 11 hpf, *tfap2c* expression is high in prospective epidermis and in the pre-placodal region (Fig. 1E). To learn whether *tfap2c* is expressed in pre-migratory neural crest at this stage, we processed embryos to reveal *foxd3* in red and *tfap2c* in blue. At 11 hpf, the most caudal *foxd3* expressing cells in the neural crest domain are found to also express *tfap2c*, while most of the rostral *foxd3* expressing cells do not express high-level *tfap2c* (Fig. 1F,F′,F″,H). Because*foxd3* expression appears in a rostral to caudal wave, these results suggest that neural crest cells down-regulate *tfap2c* expression shortly after they begin to express *foxd3*. To assess whether there is low level *tfap2c* expression in the more rostral neural crest cells, i.e., which may have been obscured by *foxd3* expression in double-labeled embryos, we processed embryos at the same stage for *tfap2c* and *sox2*, a marker of the neural plate (Okuda et al., 2006). In *tfap2c/sox2* double-labeled embryos, cells immediately flanking the cranial neural plate, which are neural crest cells, are devoid of detectable labeling (Fig. 1G). This indicates that *tfap2c* expression in neural crest has been down regulated below detectable levels at this stage. At 24 hpf, *tfap2c* expression is detected in a punctate pattern in the epidermis, but not in migrating neural crest (Fig. 1I,J). At 36 hpf, *tfap2c* expression is reduced or absent in surface ectoderm (Fig. 1K), and at 48 hpf, high level *tfap2c* expression is detected in the eye (Fig. 1L). In summary, *tfap2c* is expressed in non-neural ectoderm at gastrula stages through at least 24 hpf, and transiently in pre-migratory neural crest.

Simultaneous reduction of Tfap2a and Tfap2c has non-additive effects

To determine whether Tfap2c is required for early zebrafish development, we injected embryos with an antisense morpholino oligonucleotide (MO) targeting the *tfap2c* exon 3 splice donor site (i.e., *e3i3* MO) (Fig. 2A). RT-PCR and sequencing of the major aberrant splice product revealed that *e3i3* MO causes a deletion of 38 nucleotides, resulting in a frame shift and a severe truncation of the predicted protein, eliminating the DNA binding domain (Fig. 2A,B). However, wild-type zebrafish embryos injected with this *tfap2c* MO developed with normal morphology, pigmentation, and craniofacial cartilage (Fig. 2E, 3C,G).

The similar expression patterns of *tfap2a* and *tfap2c* in early embryos, and the similar binding specificity of Tfap2a and Tfap2c in mammals (Bosher et al., 1996;McPherson and Weigel, 1999) and amphibians (Zhang et al., 2006), suggested that Tfap2a might compensate for lack of Tfap2c in embryos injected with *tfap2c* MO. To test this model, we injected embryos derived from *tfap2a* heterozygous parents with *tfap2c e3i3* MO. One fourth of the embryos in this clutch showed striking defects, detailed below, and a PCR-based genotyping assay confirmed that the severely-affected embryos were the *tfap2a* homozygous mutants (Genotyping data presented in Supplementary Fig. S1) (100% of the *tfap2a* mutants, n = 7, and 0% of the wild-type and heterozygous siblings, n= 24, displayed the morphological phenotypes described below). By contrast, *tfap2a* mutants injected with a control MO were indistinguishable from uninjected *tfap2a* mutants. To confirm that *tfap2c e3i3* MO-induced phenotypes resulted from effects on the *tfap2c* transcript, rather than on an alternative transcript with fortuitous sequence similarity, we designed an independent MO targeting the exon 4 splice acceptor site of the *tfap2c* gene (i.e., *i3e4* MO). We performed RT-PCR and found that the *i3e4* MO also disrupted *tfap2c* splicing (Fig. 2B). Injection of *tfap2c i3e4* MO into wild-type embryos had no effect on morphology, but in one fourth of embryos derived from *tfap2a* heterozygous parents, it caused the array of phenotypes described below (7 of 30 *i3e4* MO-injected embryos, not shown). 10 of 12 embryos co-injected with *tfap2a* MO and *tfap2c* MO also showed the same morphological features (Supplementary Fig. S1). These findings suggest Tfap2a and Tfap2c have partially redundant function in zebrafish embryogenesis.

We observed a range of morphological defects in live *tfap2a* homozygous mutant embryos injected with *tfap2c e3i3* MO (hereafter, *tfap2a*$^{-}$/*c*^{MO} embryos). *tfap2a*$^{-}$/*c*^{MO} embryos can be readily distinguished from siblings by 20 hpf based on a lack of the yolk extension (not shown). In *tfap2a*$^{-}$/*c*^{MO} embryos at 28 hpf the yolk extension and tail were foreshortened, and an edema was present ventral to the pharyngeal arches (Fig. 2F,L). Lens and olfactory placodes were either not detectable or highly reduced in size, and the retinas exhibited abnormal morphology (Fig. 2H,J); these structures appeared normal in control MO-injected wild-type or *tfap2a* mutant embryos (Fig. 2G,I, and not shown). Otic vesicles in *tfap2a*$^{-}$/*c*^{MO} embryos were highly reduced in size, but always discernible, and usually contained a single otolith (Fig. 2L). Otic vesicles in control embryos and *tfap2a* mutants virtually always contained two otoliths at this stage (Fig. 2K and not shown) (Solomon and Fritz, 2002). Medial fin folds, which are derived from epidermis and contain mesenchymal cells of neural crest origin (Smith et al., 1994), were normal in control MO-injected wild type (Fig. 2M) and *tfap2a* mutant embryos (not shown), but were severely shrunken in *tfap2a*$^{-}$/*c*^{MO} embryos (Fig. 2N). Pectoral fins, which also appeared normal in *tfap2a* mutants (Fig 3 F), were reduced or absent in *tfap2a*$^{-}$/*c*^{MO} embryos (Fig. 3H). In control MO-injected *tfap2a* mutants, melanophores and iridophores were moderately reduced in number, and xanthophores were present (Fig. 3B and not shown) (Knight et al., 2004); by contrast, *tfap2a*$^{-}$/*c*^{MO} embryos lacked pigment cells of all types (Fig. 3D, and not shown). In *tfap2a* mutant embryos, cartilages derived from the hyoid arch (arch 2) and the ceratobranchial arches (arches 3–7) were reduced to various extents, whereas cartilage elements derived from the first arch (Meckel's and palatoquadrate) were relatively unaffected (Barrallo-Gimeno et al., 2004;Knight et al., 2003) (Fig. 3F). By contrast, in

tfap2a^{-}/*c*^{MO} embryos cartilage from all arches was absent, while the posterior neurocranium, which is mesoderm-derived, remained (Fig. 3H,J). In summary, wild-type embryos injected with *tfap2c* MO developed normally until at least 4 dpf, while *tfap2a*$^{-}$/*c*^{MO} embryos displayed defects far exceeding those detected in *tfap2a* mutants.

Neural crest derivatives are absent, and placode derivatives reduced in *tfap2a/c*-deficient embryos

We assessed the presence of other neural crest and placode derivatives by virtue of characteristic gene expression. Neurons of cranial ganglia are derived from both of these precursor populations (D'Amico-Martel and Noden, 1983). In *tfap2a* mutants, there is severe reduction or loss of neurons in epibranchial, distal enteric, and anterior lateral line ganglia, a more modest reduction of neurons in trigeminal and dorsal root ganglia, and apparently normal numbers of neurons in posterior lateral-line, vagal, and sympathetic ganglia (Barrallo-Gimeno et al., 2004;Holzschuh et al., 2003). In *tfap2a*$^{-}$/*c*^{MO} embryos, there was a more extreme loss of neurons in peripheral ganglia, such that trigeminal, vagal, sympathetic, proximal enteric, and dorsal root ganglia were all highly reduced in size or absent (Fig. 4B,D,F,H,J). Neural crest-derived glial cells –including satellite cells in cranial ganglia and Schwann cells associated with lateral line processes, both of which are characterized by *foxd3* expression (Kelsh et al., 2000)– were completely absent from *tfap2a*$^{-}$/*c*^{MO} embryos (Fig. 4L,N). The migrating lateral line primordium, which is placode derived, was absent from *tfap2a*$^{-}$/*c*^{MO} embryos at 28 hpf, as determined by *eya1* expression (Kozlowski et al., 2005) (Fig. 4P). Neuromasts, which derive from the lateral-line primoridium and can be detected by DASPEI labeling of hair cells, were absent in *tfap2a*$^{-}$/*c*^{MO} embryos at 3 dpf (Fig. 4R) (Harris et al., 2003). Finally, consistent with abnormal olfactory placode morphology (Fig. 2H), *eya1* expression in olfactory placode was highly reduced in *tfap2a*$^{-}$/*c*^{MO} embryos at 28 hpf (Fig. 4T). In summary, neural crest derivatives were absent in *tfap2a*$^{-}$/*c*^{MO} embryos, and placode derivatives were absent or severely reduced in size.

Simultaneous reduction of Tfap2a and Tfap2c eliminates the neural crest but not the pre-placodal domain

We speculated that redundant activity of Tfap2a and Tfap2c (hereafter referred to as Tfap2a/c activity) was required for induction or maintenance of neural crest. In *tfap2a* mutants, expression of *dlx2* in migratory neural crest is highly reduced in all but the first pharyngeal arch; however, early expression of most neural crest markers appears to be normal, except *crestin* expression is absent and *foxd3* expression is reduced specifically in hindbrain neural crest (Knight, et al. 2003). In *tfap2a*$^{-}$/*c*^{MO} embryos, we found expression of *dlx2* and *sox10* in migratory neural crest was absent in the trunk and in all pharyngeal arches (Fig. 5B,D). In addition, *foxd3* expression at 11 hpf in premigratory neural crest was absent from about one fourth of a clutch of embryos derived from *tfap2a* heterozygous parents and injected with *tfap2c e3i3* MO (7 of 26 embryos, not shown). To facilitate further evaluation of *tfap2a/c*-deficient embryos at early stages, we employed a morpholino targeting the exon 2 donor site of *tfap2a* (i.e., *tfap2a e2i2* MO). We have previously shown that embryos injected with this MO closely resemble *tfap2a* homozygous mutant embryos (O'Brien et al., 2004). We found that embryos injected with both *tfap2a e2i2* MO and *tfap2c e3i3* MO (hereafter, *tfap2a*^{MO}/*c*^{MO} embryos) recapitulate all of the morphological features of *tfap2a*$^{-}$/*c*^{MO} embryos (95%, n = 100 embryos, not shown). Expression of *foxd3*, *sox9b*, *sox10*, and *snai1b* in pre-migratory neural crest was eliminated in *tfap2a*^{MO}/*c*^{MO} embryos (Fig. 5, Supplementary Fig. S2, and not shown). By contrast, expression of the neural plate border markers *pax3*, *msxb*, and *zic2b* was normal in *tfap2a*^{MO}/*c*^{MO} embryos (Fig. 5 and not shown), and in all embryos derived from *tfap2a* heterozygous parents and injected with *tfap2c e3i3* MO (not shown, n = 40 or more embryos examined for each gene). These findings implicate Tfap2a/c activity in neural crest

induction, and place it in parallel to or possibly downstream of Pax3, Zic2b, and Msxb, and upstream of Foxd3, Sox9, Sox10, and Snai1b activities.

The defects in the sensory placodes of *tfap2a*$^{-}$/*c*^{MO} embryos suggested a failure in specification of the pre-placodal domain. However, the expression of *dlx3b* and *eya1* genes, which are both markers of the pre-placodal domain in wild-type embryos (Akimenko et al., 1994;Kozlowski et al., 2005), was normal in *tfap2a*^{MO}/*c*^{MO} embryos (Fig. 5N and Supplementary Fig. S2) and all *tfap2c* MO-injected embryos derived from *tfap2a* heterozygous parents (not shown, n = 40 or more embryos or each gene). These results suggest that Tfap2a/c activity is required for a step, or steps, that occur during the development of placodal derivatives subsequent to the establishment of the pre-placodal domain.

Rohon-Beard sensory neurons are reduced but not absent in *tfap2a/c* deficient embryos

Rohon-Beard sensory neurons (RBs) reside in the dorsal spinal cord but derive from the same neural plate domain as neural crest (Cornell and Eisen, 2000; see also Jacobson, 1991). Mutants with defective Delta/Notch signaling have supernumerary RBs but lack trunk neural crest, suggesting that RBs derive from precursor cells that are also competent to become trunk neural crest, i.e., RB/NC precursors (Cornell and Eisen, 2000;Cornell and Eisen, 2002). These data suggest the default fate for RB/NC precursors is RB, but when RB/NC precursors are exposed to the cell-surface ligand Delta, which is expressed on nascent RBs, they adopt the alternate fate of neural crest. Inhibition of *ngn1* in Delta/Notch pathway mutants will substitute for Delta signaling in RB/NC precursors, thereby eliminating RBs and restoring trunk neural crest in these mutants (Cornell and Eisen, 2002).

RBs were reported to be slightly reduced in *tfap2a* mutants (Knight et al., 2004), and our expectation was that like neural crest they would be absent from *tfap2a/c* deficient embryos. RBs are characterized by expression of *tlxA* at 20 hpf (Andermann and Weinberg, 2001). We injected control MO or *tfap2c* MO into embryos derived from *tfap2a* heterozygotes, fixed and processed embryos at 20 hpf, and counted *tlxA*-positive cells. We found that *tfap2a*$^{-}$/*c*^{MO} embryos, which could be recognized by their characteristic morphology, contained about 60% of the average number of RBs in control MO-injected embryos, i.e., both *tfap2a* mutants and their siblings (*tfap2a* mutants could not be un-ambiguously identified based on their phenotype of reduced RBs) (Fig. 6 A–C). To confirm that reduction of Tfap2a/c activity has a more severe impact on neural crest cells than RBs, we processed 12 hpf embryos derived from *tfap2a* heterozygous parents injected with *tfap2c* MO to reveal *foxd3* mRNA and anti-Islet IR (a marker of RBs) simultaneously. One fourth of these, presumed to be *tfap2a*$^{-}$/*c*^{MO} embryos, were completely devoid of *foxd3* expression (Fig. 6E), yet had residual RBs (Fig. 6E,E′). The transcription factor Prdm1/Blimp1 is implicated in the early development of neural crest and RBs (Artinger et al., 1999;Hernandez-Lagunas et al., 2005;Roy and Ng, 2004). In contrast to neural crest marker expression, which was absent, and neural plate border expression, which was normal, *prdm1* expression was highly reduced but not completely absent in *tfap2a*^{MO}/*c*^{MO} embryos (not shown) and in about one fourth of embryos derived from *tfap2a* heterozygous parents injected with *tfap2c* MO (Fig. 6 G,G′). These findings are consistent with *prdm1* being expressed in Tfap2a/c-dependent RB/NC precursors, and in a previously unknown cell type, Tfap2a/c-independent RB precursor cells (Fig. 10, see Discussion).

We considered that the presence of RBs and *prdm1* expression in *tfap2a/c*-deficient embryos might merely reflect incomplete suppression of Tfap2a/c activity. Residual Tfap2a/c activity might suffice to promote induction of a few RB/NC precursors. If these were sparsely distributed they might not receive a Delta signal and therefore would be expected to adopt the RB fate. A prediction of this model is that the number of RBs present should be highly dependent on the thoroughness of the knockdown of *tfap2a* and *tfap2c*. To test this prediction, we used *tfap2a* mutants and injected either twice (5 ng) or 4 times (10 ng) the amount of *tfap2c*

e3i3 MO necessary to eliminate *foxd3* expression (2.5 ng), and counted RBs at 20 hpf. The number of RBs in *tfap2a* mutants injected with either dose of *tfap2c* MO was the same (Fig. 6C), i.e., about 60% of the number present in control embryos, arguing against the possibility that poor distribution of *tfap2c* MO explains the presence of residual RBs in *tfap2a*$^{-}$/*c*^{MO} embryos. A second prediction of the model that RBs in *tfap2a/c* deficient embryos derive from RB/NC precursors that fail to receive a Delta signal is that inhibition of *ngn1* should convert these residual RBs to neural crest. We injected *ngn1* MO (*ngn1* MO) and *tfap2c* MO into embryos derived from *tfap2a* mutant parents. At 12 hpf, as expected, all such embryos lacked *isl1* expression in lateral neural plate, reflecting the requirement for Ngn1 in RB development (Fig. 6J) (Andermann et al., 2002;Cornell and Eisen, 2002). Significantly, one fourth of similarly treated embryos utterly lacked *foxd3* expression, that is, we did not observe expression of *foxd3* in place of RBs as predicted by this model (Fig 6M). Together these results argue against the possibility that residual RBs in *tfap2a/c* deficient embryos are derived from RB/NC precursors.

An alternative model is that there are distinct subsets of RBs, i.e., Tfap2a/c-dependent and -independent subsets. Genetically distinct subsets of RBs might be expected to have distinct expression profiles; specifically, the Tfap2a/c-independent subset might never express *tfap2a*. Consistent with this possibility, in 12.5 hpf embryos processed to reveal anti-Islet IR and *tfap2a* mRNA we detected unambiguous examples of Islet-IR-positive RBs that expressed *tfap2a* and those that did not (Fig. 6N). This result supports the existence of a Tfap2a/c-independent class of RBs (See Discussion).

Requirement for Tfap2a/c in neural crest induction is cell autonomous

To determine whether the requirement for Tfap2a/c in neural crest induction is cell-autonomous, we created genetic chimeras with blastula transplants. First, we transplanted cells from 4 hpf wild-type donors injected with a lineage tracer into wild-type host embryos. At 12 hpf, we processed embryos to reveal the lineage tracer in brown and *foxd3* expression in blue. Double-labeled donor-derived cells were readily distinguished from host-derived cells expressing *foxd3* singly (Fig. 7A,A′). Next, we repeated this experiment but used host embryos born of *tfap2a* heterozygous parents and injected with *tfap2c* MO. In *tfap2a*$^{-}$/*c*^{MO} hosts at 12hpf, which were identified by a severe reduction of *foxd3* expression, all cells expressing *foxd3* were donor-derived (with one exception out of the 151 *foxd3*-expressing cells scored) (Fig. 7B,B′). In similar chimeras grown to 48 hpf, made with wild-type donors and *tfap2a*^{MO}/*c*^{MO} hosts, virtually all melanophores were found to contain lineage tracer (Fig. 7 D,D′). These findings indicate that bona fide neural crest can develop from wild-type cells that are flanked by *tfap2a/c*-deficient non-neural ectoderm. We conducted the same experiment in reverse, using *tfap2a*$^{-}$/*c*^{MO} donors (determined by raising donors to 28 hpf after the transplant procedure) and wild-type hosts. In such chimeras, donor-derived cells were never found to express *foxd3* (Fig. 7C,C′), and in similar experiments, using a host strain that lacks melanophores to facilitate identification of donor-cell derived melanophores, *tfap2a/c*-deficient donor cells were never found to become melanophores (Supplementary Fig. S3). These results show that even when flanked by wild-type non-neural ectoderm, Tfap2a/c deficient cells were not competent to become neural crest. Together these transplant studies strongly support a cell-autonomous requirement for Tfap2a/c activity in neural crest induction.

Tfap2a/c required for neural crest specification

An absence of neural crest in *tfap2a/c*-deficient embryos was consistent with several possible roles for Tfap2a/c activity in neural crest development, including promotion of neural crest survival, proliferation, specification, or a combination of these. To test for a role for Tfap2a/c in neural crest survival, we fixed control and *tfap2a*^{MO}/*c*^{MO} embryos at 11 hpf and processed them for TUNEL, a marker of apoptotic cell death. We did not detect a gross increase in

TUNEL-positive cells in *tfap2a*^{MO}/*c*^{MO} embryos(Fig. 8A,B), although we recognized that a small or highly localized increase in TUNEL-positive cells might have been difficult to detect. Therefore, we incubated control and *tfap2a*^{MO}/*c*^{MO} embryos in the pan-caspase inhibitor, zVAD-fmk (Hsieh et al., 2003;Williams et al., 2000). We found this treatment drastically reduced levels of cell death in both populations, but it did not rescue *foxd3* expression in the latter (Fig. 8C–F). We conclude that excessive cell death is unlikely to account for the absence of neural crest in *tfap2a/c*-deficient embryos.

To test for a role for Tfap2a/c in promoting proliferation, we used BrdU incorporation to label cells in S-phase in *tfap2a*^{MO}/*c*^{MO} embryos. Because neural crest is not detectable in these embryos, we counted BrdU-positive cells in non-neural ectoderm, which expresses *tfap2a* and *tfap2c*. We did not detect a significant difference in the number of BrdU-labeled cells between control and *tfap2a*^{MO}/*c*^{MO} embryos (Fig. 8 G,H). While it is possible that Tfap2a/c is required for proliferation of neural crest, we note that if this were its only function in neural crest, we would have expected *tfap2a/c* deficient cells to express *foxd3* when transplanted into the neural crest domain of control embryos, which was not observed (Fig. 7C,C′).

We reasoned that if Tfap2a/c activity was required for neural crest specification, prospective neural crest cells would adopt an alternative fate in *tfap2a/c*-deficient embryos. We found that wild-type embryos fixed at 11 hpf and processed to reveal *sox2*, a marker of the neural plate (Okuda et al., 2006), and *dlx3b*, a marker of the preplacodal domain (Akimenko et al., 1994), exhibit a patch of unlabeled cells between these two expression domains which we presume to be neural crest (Fig. 8I,I′). However, in *tfap2a*^{MO}/*c*^{MO} embryos, this space is absent (Fig. 8J,J′). Because *dlx3b* expression is unchanged in *tfap2a*^{MO}/*c*^{MO} embryos (Fig. 5N), this finding suggests that presumptive neural crest converts to neural plate in *tfap2a/c*-deficient embryos, and thus that Tfap2a/c activity is necessary to assign ectoderm cells to the neural crest lineage.

Overexpression of *tfap2a* induces ectopic neural crest

As a positive test of the ability of Tfap2-type activity to induce neural crest we conducted a misexpression experiment. We found that injection of RNA encoding full-length Tfap2a into *tfap2a*^{MO}/*c*^{MO} embryos efficiently rescued *foxd3* expression at 11 hpf (Supplementary Fig. S4). Injection of *tfap2a* mRNA into wild-type embryos expanded neural crest expression of *foxd3* (not shown), although abnormal gastrulation in these embryos complicated interpretation of this finding. To circumvent the effect of ectopic Tfap2a on gastrulation, we injected RNA encoding an dexamethasone-inducible form of *X. laevis* Tfap2a, *GRXAP2* (Luo et al., 2005), added dexamethasone at mid-gastrulation (6 hpf), fixed embryos at 11 hpf, and processed them to reveal expression of *foxd3* or other early markers of premigratory neural crest. In such embryos, which appeared to undergo gastrulation normally, we detected ectopic expression of *foxd3, snai1b, sox9b*, and *sox10* in the neural plate (Fig. 9B,D,F, and not shown), and reduced expression of neural plate marker *sox2* (Fig. 9H). Moreover, when such embryos were allowed to develop to 36 hpf, they often displayed patches of supernumerary melanophores (Fig. 9J), possibly resulting from a conversion of neural plate to neural crest, although abnormal growth within the melanophore lineage would also explain this finding. The results of these gain-of-function experiments are consistent with a requirement for Tfap2a/c in neural crest induction.

Discussion

Requirement for Tfap2-type activity in neural crest induction is conserved

Our data reveal that Tfap2a and Tfap2c function redundantly in neural crest induction and in development of other non-neural ectoderm derivatives. While neural crest induction occurs normally in embryos deficient in *tfap2c* (present study), and largely normally in embryos deficient in *tfap2a* (Knight et al., 2003;O'Brien et al., 2004), it appears to fail altogether in

embryos deficient in both *tfap2a* and *tfap2c*. Additional phenotypes observed in *tfap2a/c*-doubly deficient embryos, but not in embryos singly deficient in either gene, include a failure of lens, ear, and olfactory placode to develop normally, and abnormal epidermal development, as revealed by shrunken medial fin folds. These phenotypes reveal that Tfap2a and Tfap2c can compensate for each other's absence in many contexts during zebrafish development. These proteins also appear to cooperate in mouse extra-embryonic tissue (Winger et al., 2006). We predict that compensatory activity of Tfap2c explains why neural crest induction occurs normally in mouse *Tcfap2a* homozygous mutants. Importantly, our results suggest that a role for Tfap2-type activity in neural crest induction is a conserved feature of vertebrate development. In fish, and possibly in mice, this role is shared between two closely related Tfap2 family members, Tfap2a and Tfap2c. In frog embryos this role is largely carried out by Tfap2a, but also possibly in part by Tfap2c because inhibition of *TFAP2A* reduces, but does not completely eliminate, neural crest (Luo et al., 2003).

Cell-autonomous Tfap2-type activity is required for neural crest induction

Many previous studies have shown that Tfap2-type activity can regulate the balance between cell proliferation and differentiation or death (reviewed in Eckert et al., 2005). The present findings, together with earlier work in frog (Luo et al., 2003), suggest that Tfap2-type activity can also govern cell fate specification, in this case, the choice of an ectodermal cell to become neural crest. Several alternative explanations for the loss of neural crest in *tfap2a/c* deficient embryos were ruled out. For instance, this loss might have resulted from conversion of posterior neural tissue to anterior, from which neural crest does not arise. Indeed, *tfap2a/c* deficient embryos display reduced extension of the tail, consistent with anteriorization of the embryo, perhaps reflecting regulation of *tfap2a* and *tfap2c* by the well-known posteriorizing factor retinoic acid (Oulad-Abdelghani et al., 1996;Wanner et al., 1996). However, arguing against a wholesale conversion of neural tissue to a rostral identity, multiple derivatives of the spinal cord are detected in *tfap2a/c* deficient embryos, including primary motoneurons, a subset of RBs, and *spt* expressing interneurons (WL and RAC, unpublished observations). In addition, changes in proliferation or cell death did not appear to be sufficient to account for the absence of neural crest in *tfap2a/c*-deficient embryos; we note that if either of these were the explanation, a change would have been expected in *msxb* expression, whose domain overlaps the neural crest (Phillips et al., 2006; RAC, unpublished observations). Rather, our observation that *sox2* is expanded in *tfap2a/c* deficient embryos suggests neural crest is converted to neural plate in such embryos. We predict that a dorsal or intermediate spinal cord fate is expanded in *tfap2a/c* deficient embryos. Although we have not yet identified such a fate, we note that in such embryos, RBs are unusually widely distributed in the medio-lateral dimension, consistent with abnormal dorso-ventral patterning of the spinal cord. It is noteworthy that Tfap2-type activity is required for epidermis-specific gene expression (Luo et al., 2002). Whether Tfap2-type activity induces neural crest or epidermis may depend on the presence of specific cofactors, or the absence of specific repressors. Msx, Pax, and Zic family members are candidates for Tfap2 co-factors during induction of neural crest specific genes (Monsoro-Burq et al., 2005).

The absence of neural crest in *tfap2a/c*-deficient embryos did not immediately reveal which tissues require Tfap2a/c expression for neural crest induction. There is strong evidence that neural crest patterning depends on Tfap2-type activity in surrounding tissues (Brewer et al., 2004;Knight et al., 2005). However, our transplant studies support a cell-autonomous requirement for Tfap2a/c during neural crest induction. Because *tfap2c* expression is rapidly down regulated in neural crest, Tfap2a/c function in neural crest induction must occur during gastrula stage. At later stages, expression of *tfap2a* members persists in migratory neural crest and many of its derivatives. The cell autonomous function of Tfap2-type activity within neural crest (i.e., subsequent to its induction) is unknown, but conceivably includes control of survival,

proliferation, or patterning. Within neural crest derivatives, Tfap2-type activity promotes *Kit* expression in melanophores (Brewer et al., 2004), *tyrosine hydroxylase* expression in sympathetic neurons (Holzschuh et al., 2003;Kim et al., 2001), and *hoxa2* expression in cranial neural crest streams (Maconochie et al., 1999). Identification of all functions mediated by Tfap2-type activity in neural crest will require simultaneous, tissue-specific knockdown of each *tfap2* family members expressed in neural crest.

A subset of RBs may be independent of Tfap2-type activity

The persistence of RBs in *tfap2a/c*-deficient embryos is consistent with several models (Fig. 10). In one, Tfap2a/c activity is required for specification of RB/NC precursors, but *tfap2a*$^{-}$/*c*^{MO} embryos have sufficient residual Tfap2a/c activity to allow induction of a few such precursors. These all adopt the RB fate because they are sparsely distributed and do not receive the Delta signal necessary to induce them to become neural crest. While we did not find the number of RBs to be highly dependent on the dose of injected *tfap2c* MO, maternally encoded Tfap2c may persist in *tfap2a*$^{-}$/*c*^{MO} embryos at sufficient levels to permit induction of some RB/NC precursors. If this were the case, however, we would have expected injection of *ngn1* MO into *tfap2a*$^{-}$/*c*^{MO} embryos to convert residual RBs to *foxd3*-positive neural crest cells, which it did not. An alternative model is that Tfap2a/c activity is not required for specification of RB/NC precursors, but rather for the subsequent specification of neural crest from these precursors (Fig. 10). Our data are consistent with this model, but we do not favor it because it does not explain the reduction of RBs in *tfap2a/c*-deficient embryos at neural plate stages. Finally, in our preferred model, a subset of RBs is derived from Tfap2a/c-dependent RB/NC precursors, and another subset is derived from Tfap2a/c-independent precursor cells, presumably present in the neural plate (NP) (i.e., an RB/NP precursor) (Fig. 10). Lineage experiments in frog embryos reveal that at least some RBs derive from a progenitor cell at the 512-cell stage that does not give rise to neural crest (referenced in Jacobson, 1991). Different subsets of RBs might be expected to have distinct expression profiles, and we found that at the 6-somite stage not all RBs expressed *tfap2a*. We cannot rule out the possibility that all RBs initially express *tfap2a* but a subset of them by 6-somite stage no longer does so. Nonetheless, it is an intriguing hypothesis that the RBs that express *tfap2a* represent the subset of RBs that derive from RB/NC precursor cells. Lineage studies correlated with gene expression analyses will be required to test this possibility.

Finally, we note that the possibility that a subset of RBs is independent of Tfap2a/c activity is consistent with an earlier proposal that RBs predate the neural crest in evolutionary terms. This hypothesis was partially based on the presence of sensory neurons in the dorsal central nervous system of *Amphioxus*, a modern cephalochordate believed to share features with the hypothesized vertebrate precursor (Bone, 1960;Fritzsch and Northcutt, 1993). Whatever the relationship between RBs and neural crest, evidence that Tfap2-type activity is a conserved requirement for neural crest induction supports the model that the emergence of neural crest during evolution required modification of the ancestral *Tfap2* gene's regulatory domain to expand *Tfap2* expression from the presumptive epidermis into the lateral neural plate (Meulemans and Bronner-Fraser, 2005).

Supplementary Material

Refer to Web version on PubMed Central for supplementary material.

Acknowledgements

RAC gratefully acknowledges assistance from Dr. Joni Kinsey, Department of Art History, University of Iowa. We thank Greg Bonde for help with embryo injections and transplant experiments, Tom Sargent, Dan Meulemans, and Kristin Artinger for helpful discussions, David Kimelman, Yi-Lin Yan, David Raible, Paul Henion, Kristin Artinger, and John Postlethwait for probes, Tom Sargent and David Turner for plasmids, and Michael Rebagliati and Kristin

Artinger for critical reading of the manuscript. The Islet antibody mAb 39.4D5, developed by Dr. Tom Jessell's laboratory was obtained from the Developmental Studies Hybridoma Bank developed under the auspices of the NICHD and maintained by The University of Iowa, Department of Biological Sciences, Iowa City, IA 52242. This work supported by a seed grant from the American Cancer Society administered by the Holden Comprehensive Cancer Care Center, a March of Dimes Beginning Grant in Aid, and NIH GM067841 to RAC.

References

Akimenko MA, Ekker M, Wegner J, Lin W, Westerfield M. Combinatorial expression of three zebrafish genes related to distal-less: part of a homeobox gene code for the head. J Neurosci 1994;14:3475–86. [PubMed: 7911517]

Andermann P, Ungos J, Raible DW. Neurogenin1 defines zebrafish cranial sensory ganglia precursors. Dev Biol 2002;251:45–58. [PubMed: 12413897]

Andermann P, Weinberg ES. Expression of zTlxA, a Hox11-like gene, in early differentiating embryonic neurons and cranial sensory ganglia of the zebrafish embryo. Dev Dyn 2001;222:595–610. [PubMed: 11748829]

Artinger KB, Chitnis AB, Mercola M, Driever W. Zebrafish narrowminded suggests a genetic link between formation of neural crest and primary sensory neurons. Development 1999;126:3969–79. [PubMed: 10457007]

Auman HJ, Nottoli T, Lakiza O, Winger Q, Donaldson S, Williams T. Transcription factor AP-2gamma is essential in the extra-embryonic lineages for early postimplantation development. Development 2002;129:2733–47. [PubMed: 12015300]

Barrallo-Gimeno A, Holzschuh J, Driever W, Knapik EW. Neural crest survival and differentiation in zebrafish depends on mont blanc/tfap2a gene function. Development 2004;131:1463–77. [PubMed: 14985255]

Bone Q. The central nervous system in Amphioxus. J Comp Neurol 1960;115:27–51.

Bosher JM, Totty NF, Hsuan JJ, Williams T, Hurst HC. A family of AP-2 proteins regulates c-erbB-2 expression in mammary carcinoma. Oncogene 1996;13:1701–7. [PubMed: 8895516]

Brewer S, Feng W, Huang J, Sullivan S, Williams T. Wnt1-Cre-mediated deletion of AP-2alpha causes multiple neural crest-related defects. Dev Biol 2004;267:135–52. [PubMed: 14975722]

Chazaud C, Oulad-Abdelghani M, Bouillet P, Decimo D, Chambon P, Dolle P. AP-2.2, a novel gene related to AP-2, is expressed in the forebrain, limbs and face during mouse embryogenesis. Mech Dev 1996;54:83–94. [PubMed: 8808408]

Cornell RA, Eisen JS. Delta signaling mediates segregation of neural crest and spinal sensory neurons from zebrafish lateral neural plate. Development 2000;127:2873–82. [PubMed: 10851132]

Cornell RA, Eisen JS. Delta/Notch signaling promotes formation of zebrafish neural crest by repressing Neurogenin 1 function. Development 2002;129:2639–48. [PubMed: 12015292]

D'Amico-Martel A, Noden DM. Contributions of placodal and neural crest cells to avian cranial peripheral ganglia. Am J Anat 1983;166:445–68. [PubMed: 6858941]

Dickinson ME, Selleck MA, McMahon AP, Bronner-Fraser M. Dorsalization of the neural tube by the non-neural ectoderm. Development 1995;121:2099–106. [PubMed: 7635055]

Eckert D, Buhl S, Weber S, Jager R, Schorle H. The AP-2 family of transcription factors. Genome Biol 2005;6:246. [PubMed: 16420676]

Fritzsch B, Northcutt RG. Cranial and spinal nerve organization in amphioxus and lampreys: evidence for an ancestral craniate pattern. Acta Anat (Basel) 1993;148:96–109. [PubMed: 8109201]

Harris JA, Cheng AG, Cunningham LL, MacDonald G, Raible DW, Rubel EW. Neomycin-induced hair cell death and rapid regeneration in the lateral line of zebrafish (Danio rerio). J Assoc Res Otolaryngol 2003;4:219–34. [PubMed: 12943374]

Hernandez-Lagunas L, Choi IF, Kaji T, Simpson P, Hershey C, Zhou Y, et al. Zebrafish narrowminded disrupts the transcription factor prdm1 and is required for neural crest and sensory neuron specification. Dev Biol 2005;278:347–57. [PubMed: 15680355]

Hilger-Eversheim K, Moser M, Schorle H, Buettner R. Regulatory roles of AP-2 transcription factors in vertebrate development, apoptosis and cell-cycle control. Gene 2000;260:1–12. [PubMed: 11137286]

Holzschuh J, Barrallo-Gimeno A, Ettl AK, Durr K, Knapik EW, Driever W. Noradrenergic neurons in the zebrafish hindbrain are induced by retinoic acid and require tfap2a for expression of the neurotransmitter phenotype. Development 2003;130:5741–54. [PubMed: 14534139]

Hong CS, Saint-Jeannet JP. Sox proteins and neural crest development. Semin Cell Dev Biol 2005;16:694–703. [PubMed: 16039883]

Hsieh YC, Chang MS, Chen JY, Yen JJ, Lu IC, Chou CM, Huang CJ. Cloning of zebrafish BAD, a BH3-only proapoptotic protein, whose overexpression leads to apoptosis in COS-1 cells and zebrafish embryos. Biochem Biophys Res Commun 2003;304:667–75. [PubMed: 12727206]

Jacobson, M. Developmental Neurobiology. Plenum Press; New York: 1991.

Kelsh RN, Dutton K, Medlin J, Eisen JS. Expression of zebrafish fkd6 in neural crest-derived glia. Mech Dev 2000;93:161–4. [PubMed: 10781949]

Kim HS, Hong SJ, LeDoux MS, Kim KS. Regulation of the tyrosine hydroxylase and dopamine beta-hydroxylase genes by the transcription factor AP-2. J Neurochem 2001;76:280–94. [PubMed: 11146001]

Kimmel CB, Ballard WW, Kimmel SR, Ullmann B, Schilling TF. Stages of embryonic development of the zebrafish. Dev Dyn 1995;203:253–310. [PubMed: 8589427]

Kimmel CB, Miller CT, Kruze G, Ullmann B, BreMiller RA, Larison KD, Snyder HC. The shaping of pharyngeal cartilages during early development of the zebrafish. Dev Biol 1998;203:245–63. [PubMed: 9808777]

Kimmel CB, Warga RM, Schilling TF. Origin and organization of the zebrafish fate map. Development 1990;108:581–94. [PubMed: 2387237]

Knight RD, Javidan Y, Nelson S, Zhang T, Schilling T. Skeletal and pigment cell defects in the lockjaw mutant reveal multiple roles for zebrafish tfap2a in neural crest development. Dev Dyn 2004;229:87–98. [PubMed: 14699580]

Knight RD, Javidan Y, Zhang T, Nelson S, Schilling TF. AP2-dependent signals from the ectoderm regulate craniofacial development in the zebrafish embryo. Development 2005;132:3127–38. [PubMed: 15944192]

Knight RD, Nair S, Nelson SS, Afshar A, Javidan Y, Geisler R, et al. lockjaw encodes a zebrafish tfap2a required for early neural crest development. Development 2003;130:5755–68. [PubMed: 14534133]

Kozlowski DJ, Whitfield TT, Hukriede NA, Lam WK, Weinberg ES. The zebrafish dog-eared mutation disrupts eya1, a gene required for cell survival and differentiation in the inner ear and lateral line. Dev Biol 2005;277:27–41. [PubMed: 15572137]

Kudoh T, Concha ML, Houart C, Dawid IB, Wilson SW. Combinatorial Fgf and Bmp signalling patterns the gastrula ectoderm into prospective neural and epidermal domains. Development 2004;131:3581–92. [PubMed: 15262889]

Lewis JL, Bonner J, Modrell M, Ragland JW, Moon RT, Dorsky RI, Raible DW. Reiterated Wnt signaling during zebrafish neural crest development. Development 2004;131:1299–308. [PubMed: 14973296]

Liem KF Jr, Tremml G, Roelink H, Jessell TM. Dorsal differentiation of neural plate cells induced by BMP-mediated signals from epidermal ectoderm. Cell 1995;82:969–79. [PubMed: 7553857]

Lister JA, Robertson CP, Lepage T, Johnson SL, Raible DW. nacre encodes a zebrafish microphthalmia-related protein that regulates neural-crest-derived pigment cell fate. Development 1999;126:3757–67. [PubMed: 10433906]

Luo T, Lee YH, Saint-Jeannet JP, Sargent TD. Induction of neural crest in Xenopus by transcription factor AP2alpha. Proc Natl Acad Sci U S A 2003;100:532–7. [PubMed: 12511599]

Luo T, Matsuo-Takasaki M, Thomas ML, Weeks DL, Sargent TD. Transcription factor AP-2 is an essential and direct regulator of epidermal development in Xenopus. Dev Biol 2002;245:136–44. [PubMed: 11969261]

Luo T, Zhang Y, Khadka D, Rangarajan J, Cho KW, Sargent TD. Regulatory targets for transcription factor AP2 in Xenopus embryos. Dev Growth Differ 2005;47:403–13. [PubMed: 16109038]

Maconochie M, Krishnamurthy R, Nonchev S, Meier P, Manzanares M, Mitchell PJ, Krumlauf R. Regulation of Hoxa2 in cranial neural crest cells involves members of the AP-2 family. Development 1999;126:1483–94. [PubMed: 10068641]

McPherson LA, Weigel RJ. AP2alpha and AP2gamma: a comparison of binding site specificity and trans-activation of the estrogen receptor promoter and single site promoter constructs. Nucleic Acids Res 1999;27:4040–9. [PubMed: 10497269]

Meulemans D, Bronner-Fraser M. Central role of gene cooption in neural crest evolution. J Exp Zoolog B Mol Dev Evol 2005;304:298–303. [PubMed: 15880502]

Mitchell PJ, Timmons PM, Hebert JM, Rigby PW, Tjian R. Transcription factor AP-2 is expressed in neural crest cell lineages during mouse embryogenesis. Genes Dev 1991;5:105–19. [PubMed: 1989904]

Moens CB, Fritz A. Techniques in neural development. Methods Cell Biol 1999;59:253–72. [PubMed: 9891364]

Monsoro-Burq AH, Wang E, Harland R. Msx1 and Pax3 cooperate to mediate FGF8 and WNT signals during Xenopus neural crest induction. Dev Cell 2005;8:167–78. [PubMed: 15691759]

Moser M, Ruschoff J, Buettner R. Comparative analysis of AP-2 alpha and AP-2 beta gene expression during murine embryogenesis. Dev Dyn 1997;208:115–24. [PubMed: 8989526]

Moury JD, Jacobson AG. The origins of neural crest cells in the axolotl. Dev Biol 1990;141:243–53. [PubMed: 2210034]

Nasevicius A, Ekker SC. Effective targeted gene 'knockdown' in zebrafish. Nat Genet 2000;26:216–20. [PubMed: 11017081]

O'Brien EK, d'Alencon C, Bonde G, Li W, Schoenebeck J, Allende ML, et al. Transcription factor Ap-2alpha is necessary for development of embryonic melanophores, autonomic neurons and pharyngeal skeleton in zebrafish. Dev Biol 2004;265:246–61. [PubMed: 14697367]

Okuda Y, Yoda H, Uchikawa M, Furutani-Seiki M, Takeda H, Kondoh H, Kamachi Y. Comparative genomic and expression analysis of group B1 sox genes in zebrafish indicates their diversification during vertebrate evolution. Dev Dyn 2006;235:811–25. [PubMed: 16408288]

Oulad-Abdelghani M, Bouillet P, Chazaud C, Dolle P, Chambon P. AP-2.2: a novel AP-2-related transcription factor induced by retinoic acid during differentiation of P19 embryonal carcinoma cells. Exp Cell Res 1996;225:338–47. [PubMed: 8660922]

Phillips BT, Kwon HJ, Melton C, Houghtaling P, Fritz A, Riley BB. Zebrafish msxB, msxC and msxE function together to refine the neural-nonneural border and regulate cranial placodes and neural crest development. Dev Biol 2006;294:376–90. [PubMed: 16631154]

Reyes R, Haendel M, Grant D, Melancon E, Eisen JS. Slow degeneration of zebrafish Rohon-Beard neurons during programmed cell death. Dev Dyn 2004;229:30–41. [PubMed: 14699575]

Roy S, Ng T. Blimp-1 specifies neural crest and sensory neuron progenitors in the zebrafish embryo. Curr Biol 2004;14:1772–7. [PubMed: 15458650]

Sahly I, Andermann P, Petit C. The zebrafish eya1 gene and its expression pattern during embryogenesis. Dev Genes Evol 1999;209:399–410. [PubMed: 10370123]

Sauka-Spengler T, Bronner-Fraser M. Development and evolution of the migratory neural crest: a gene regulatory perspective. Curr Opin Genet Dev 2006;16:360–6. [PubMed: 16793256]

Schilling TF, Piotrowski T, Grandel H, Brand M, Heisenberg CP, Jiang YJ, et al. Jaw and branchial arch mutants in zebrafish I: branchial arches. Development 1996;123:329–44. [PubMed: 9007253]

Schorle H, Meier P, Buchert M, Jaenisch R, Mitchell PJ. Transcription factor AP-2 essential for cranial closure and craniofacial development. Nature 1996;381:235–8. [PubMed: 8622765]

Selleck MA, Bronner-Fraser M. Origins of the avian neural crest: the role of neural plate-epidermal interactions. Development 1995;121:525–38. [PubMed: 7768190]

Smith M, Hickman A, Amanze D, Lumsden A, Thorogood P. Trunk neural crest origin of caudal fin mesenchyme in the zebrafish *Brachydanio rerio*. Proc R Soc Lond 1994;256:137–145.

Solomon KS, Fritz A. Concerted action of two dlx paralogs in sensory placode formation. Development 2002;129:3127–36. [PubMed: 12070088]

Steventon B, Carmona-Fontaine C, Mayor R. Genetic network during neural crest induction: from cell specification to cell survival. Semin Cell Dev Biol 2005;16:647–54. [PubMed: 16084743]

Thisse B, Pflumio S, Furthauer M, Loppin B, Heyer V, Degrave A, et al. Expression of the zebrafish genome during embryogenesis. ZFIN Direct Data Submission, NIH RO1 RR15402. 2001

Thisse C, Thisse B, Postlethwait JH. Expression of snail2, a second member of the zebrafish snail family, in cephalic mesendoderm and presumptive neural crest of wild-type and spadetail mutant embryos. Dev Biol 1995;172:86–99. [PubMed: 7589816]

Wanner R, Zhang J, Henz BM, Rosenbach T. AP-2 gene expression and modulation by retinoic acid during keratinocyte differentiation. Biochem Biophys Res Commun 1996;223:666–9. [PubMed: 8687453]

Werling U, Schorle H. Transcription factor gene AP-2 gamma essential for early murine development. Mol Cell Biol 2002;22:3149–56. [PubMed: 11940672]

Westerfield, M. The Zebrafish Book. University of Oregon Press; Eugene, OR: 1993.

Williams JA, Barrios A, Gatchalian C, Rubin L, Wilson SW, Holder N. Programmed cell death in zebrafish rohon beard neurons is influenced by TrkC1/NT-3 signaling. Dev Biol 2000;226:220–30. [PubMed: 11023682]

Winger Q, Huang J, Auman HJ, Lewandoski M, Williams T. Analysis of transcription factor AP-2 expression and function during mouse preimplantation development. Biol Reprod 2006;75:324–33. [PubMed: 16672719]

Yan YL, Willoughby J, Liu D, Crump JG, Wilson C, Miller CT, et al. A pair of Sox: distinct and overlapping functions of zebrafish sox9 co-orthologs in craniofacial and pectoral fin development. Development 2005;132:1069–83. [PubMed: 15689370]

Zhang J, Hagopian-Donaldson S, Serbedzija G, Elsemore J, Plehn-Dujowich D, McMahon AP, et al. Neural tube, skeletal and body wall defects in mice lacking transcription factor AP-2. Nature 1996;381:238–41. [PubMed: 8622766]

Zhang Y, Luo T, Sargent TD. Expression of TFAP2beta and TFAP2gamma genes in Xenopus laevis. Gene Expr Patterns 2006;6:589–95. [PubMed: 16414310]

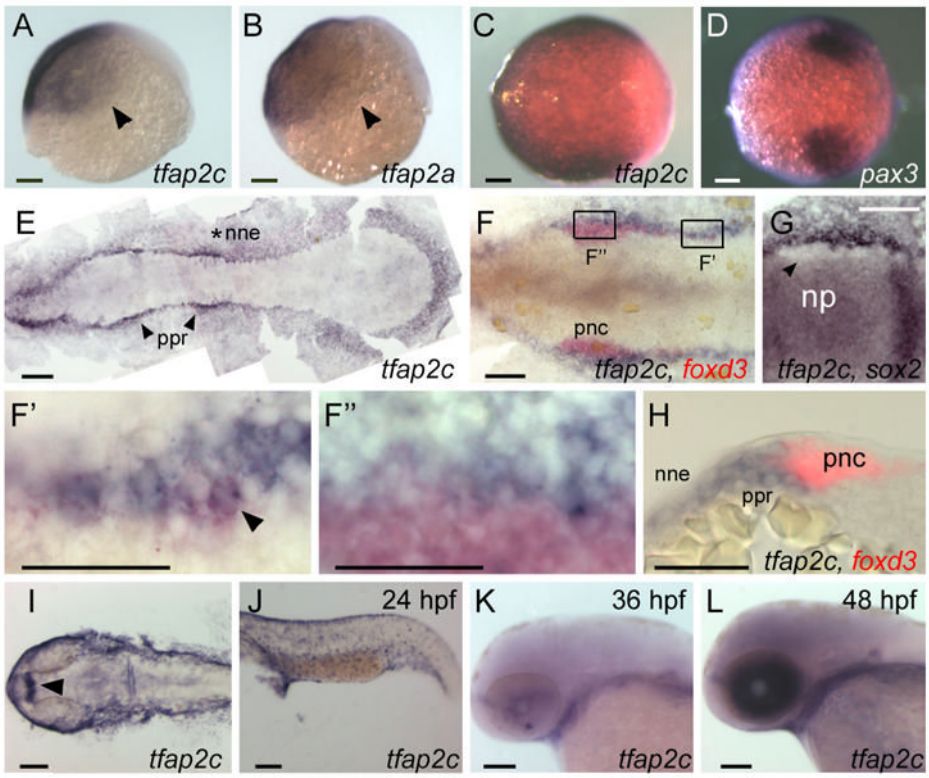

Figure 1.

Comparison of *tfap2a* and *tfap2c* expression at embryonic stages. **A, B** Lateral views, animal pole oriented up and dorsal side to the right, of **A**, *tfap2c* and **B**, *tfap2a* expression in ventral and lateral ectoderm at 6 hpf. Arrowheads point to the limit of expression, which is similar or identical for the genes. **C**, **D** Animal pole views of **C**, *tfap2c* and **D**, *pax3* expression at 8.5 hpf. Expression of *pax3* marks prospective neural crest (Lewis et al., 2004); *tfap2c* expression partially or entirely overlaps it. **E–G** Dorsal views of flat-mounted embryos at 11 hpf, anterior to the left. **E** *tfap2c* expression is detected in non-neural ectoderm (nne, asterisk), with increased levels immediately adjacent to the rostral neural plate, in the pre-placodal region (ppr, arrowheads). **F** Double RNA in situ hybridization with *foxd3* (red) and *tfap2c* (blue) probes. More caudal cells expressing *foxd3*, which are recently specified pre-migratory neural crest cells (pnc), also express *tfap2c* (shown at higher magnification in **F′**, arrowhead indicates double-labeled cell). By contrast, at more rostral levels, *tfap2c* is expressed in ppr but is excluded from the majority of *foxd3* expressing cells (shown at higher magnification in **F″**). **G** An embryo labeled with *tfap2c* and *sox2*, a pan-neural plate marker (Okuda et al., 2006). *tfap2c* expression is absent from cells immediately lateral to the neural plate, which is the pnc domain (arrowhead). **H** A transverse section of an embryo labeled as in **F**. *tfap2c* (blue) is expressed at high level in the ppr and nne, lateral to *foxd3* expression (red) in pnc. **I–L** Dorsal and lateral views of embryos at the indicated ages processed to reveal *tfap2c*. **I** In the head, and **J**, trunk at 24 hpf, expression of *tfap2c* is detected in surface ectoderm and diencephalon (arrowhead). **K** At 36hpf, *tfap2c* expression is reduced in surface ectoderm; **L** at 48 hpf, high level *tfap2c* expression is detected in the eye. Scale bars: **A–G**, **I–L**, 100 microns; **F′–H**, 50 microns.

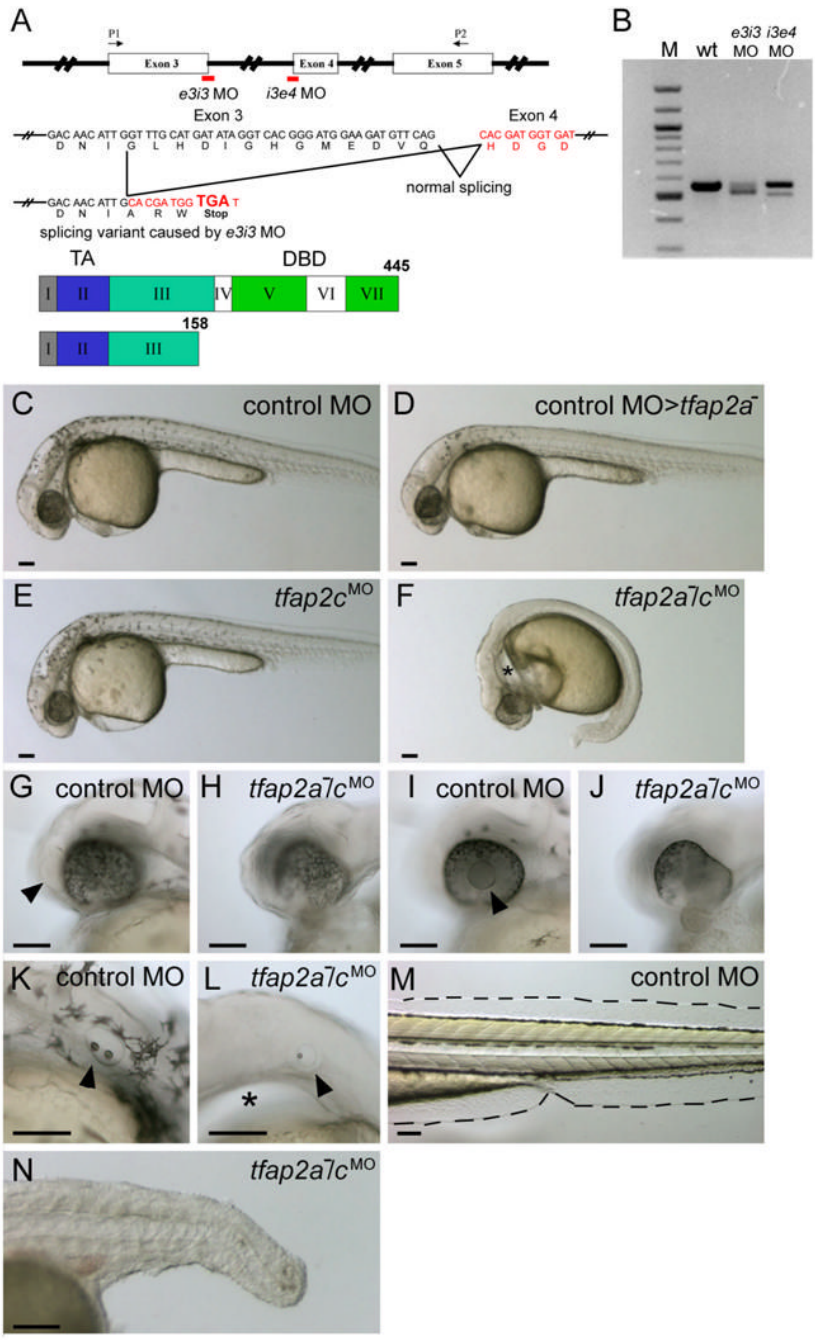

Figure 2.

tfap2a mutant embryos injected with *tfap2c* morpholino (MO) display abnormal development in ectoderm-derived tissues. **A** Top, schematic of the *tfap2c* gene showing the position of MOs used in this study; middle, effects of the *tfap2c e3i3* MO on the *tfap2c* transcript; bottom, the Tfap2c protein. Roman numerals refer to exons, numbers refer to amino acids. TA, transactivation domain. DBD, DNA binding domain. *e3i3* MO targeting the exon 3 splice donor site and *i3e4* MO targeting the exon 4 splicing acceptor site are shown in red. P1 and P2 are the primers used for the RT-PCR shown in **B**. *tfap2c e3i3* MO causes a deletion of 38 nucleotides, which leads to a frame shift and introduces a stop codon at the end of exon 3. **B** *tfap2c* RT-PCR results. Amplification of cDNA from uninjected wild-type embryos (wt) with

the primers P1 and P2 shown in **A** yielded a single band of the expected size of 557 bp, while amplification of 24 hpf cDNA from *tfap2c e3i3* MO injected embryos (*e3i3* MO) yielded a smaller band of 519 bp. Amplification of cDNA from *tfap2c i3e4* MO injected embryos (*i3e4* MO) also yielded a smaller band. M, 100 bp ladder. **C**–**F** Lateral views of live embryos at 28 hpf. In **C**, a wild-type embryo injected with standard control MO (hereafter, control embryo) with normal morphology and pigmentation. In **D**, a control MO-injected *tfap2a* homozygous mutant embryo displaying normal morphology but reduced number of melanophores. In **E**, a wild-type embryo injected with *tfap2c e3i3* MO with normal morphology and pigmentation. **F** A *tfap2a* homozygous mutant embryo injected with *tfap2c e3i3* MO (hereafter, $tfap2a^{-}/c^{MO}$ embryo), with no visible pigmentation, an absence of yolk extension, a poorly extended tail, and edema ventral to the hindbrain (asterisk). **G**–**L** Lateral views of the embryos shown in **C** and **F** at higher magnification. Olfactory placode (arrowhead in **G**) and lens (arrowhead in **I**) are visible in the control embryo but not in the $tfap2a^{-}/c^{MO}$ embryo (**H, J**) which also displays malformation of the ventral retina. Otic vesicle in **K**, the control embryo, contains two otoliths (arrowhead). While in **L**, the $tfap2a^{-}/c^{MO}$ embryo, it is reduced in size and contains a single otolith (arrowhead). An enlarged view of the edema ventral to the hindbrain is also seen (asterisk). **M, N** Lateral views of the same embryos shown in **C** and **F** at 72 hpf. Medial fin folds, as outlined in **M**, the control embryo, are virtually absent in **N**, the $tfap2a^{-}/c^{MO}$ embryo. Notochord and somites also appear abnormal, presumably due to indirect effects, because *tfap2a* and *tfap2c* expression are not detected in these tissues. Scale bars: 100 microns.

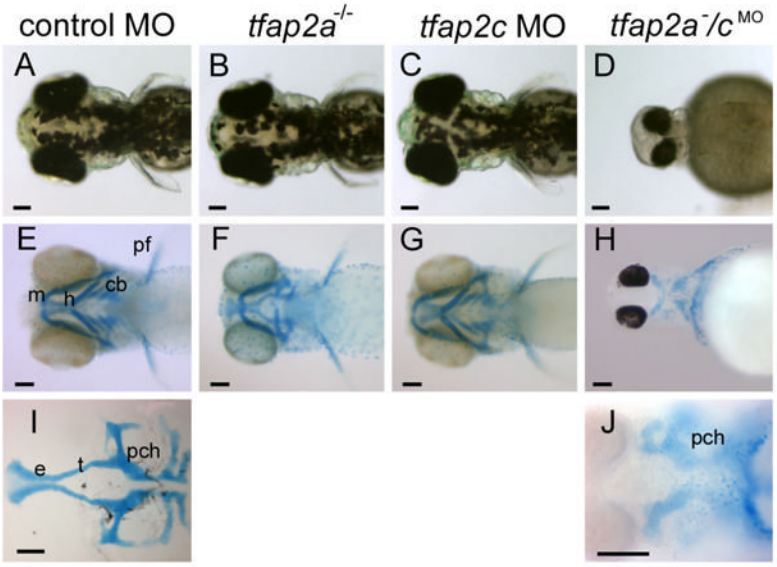

Figure 3.

tfap2a/c deficient embryos display non-additive defects in pigmentation and jaw morphology. **A–D** Dorsal views of live 72 hpf embryos. **A** Melanophores are abundant on the dorsal aspect of the head in a control-MO injected wild-type embryo, slightly reduced in **B**, a control MO-injected *tfap2a* mutant, normal in **C**, a *tfap2c* MO-injected wild-type embryo, but absent from **D**, a *tfap2a*$^{-}$/*c*^{MO} embryo (6 of 6 *tfap2a*$^{-}$/*c*^{MO} embryos). **E–H** Ventral views of 4 dpf embryos processed to reveal cartilage (alcian green), and bleached to remove pigment (except **H**). **E** Cartilages derived from mandibular (1st arch, m), hyoid (2nd arch, h), and ceratobranchial (3rd–7th arches, cb) arches are seen in a control embryo. Pectoral fin (pf) is also visible. **F** A control MO-injected *tfap2a* homozygous mutant embryo, with normal sized mandibular, but severely reduced hyoid and ceratobranchial cartilages, as previously reported (Schilling et al., 1996). **G** A *tfap2c* MO-injected wild-type embryo, in which all craniofacial cartilages appear normal. **H** A *tfap2a*$^{-}$/*c*^{MO} embryo, in which ventral craniofacial cartilage elements and pectoral fin are absent (10 of 10 *tfap2a*$^{-}$/*c*^{MO} embryos). **I** Ventral view of dissected neurocranium from a control embryo. **J** Ventral view of a *tfap2a*$^{-}$/*c*^{MO} embryo, shown at higher magnification, only the mesoderm-derived posterior neurocranium is visible (10 of 10 *tfap2a*$^{-}$/*c*^{MO} embryos). e, ethmoid plate; pch, parachordal; t, trabeculae cranii (Schilling et al., 1996). Scale bars: 100 microns.

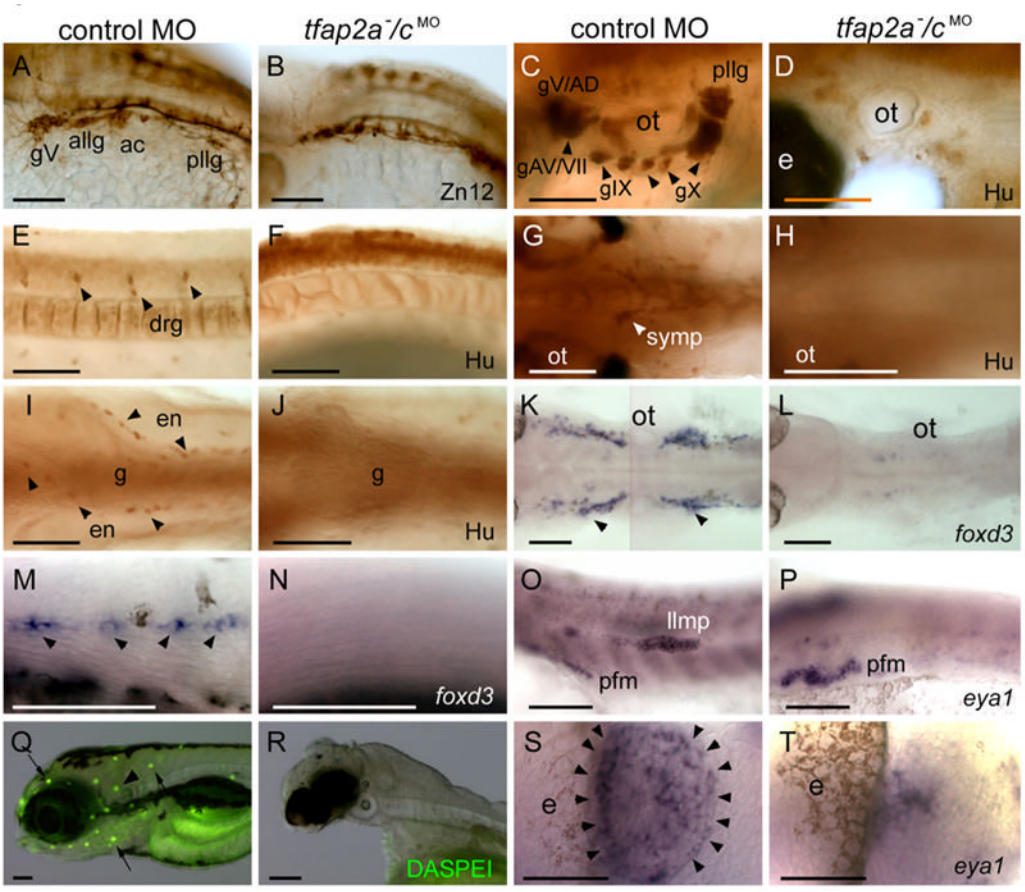

Figure 4.

Neural crest and placode derivatives are absent or reduced in *tfap2a/c* deficient embryos. **A, B** Lateral views of 28 hpf embryos processed for anti-HNK1 (Zn12 antibody) immunoreactivity (IR), revealing the presence of cranial ganglia neurons in **A**, a control MO injected wild-type embryos, and their absence in **B**, a *tfap2a*$^{-}$/*c*^{MO} embryo (9 of 10 *tfap2a*$^{-}$/*c*^{MO} embryos). **C–F** Lateral and **G–J** ventral views of 72 hpf embryos processed for anti-Hu IR. **C, E, G, I** In control embryos anti-Hu IR reveals **C**, cranial ganglia surrounding the otic vesicle (ot), **E**, dorsal root ganglia (drg) in the trunk, **G**, sympathetic neurons at vagal level, and **I**, proximal enteric neurons, adjacent to gut (g), also at vagal level. **D, F, H, J** All of these neurons appear to be absent from a *tfap2a*$^{-}$/*c*^{MO} embryo (8 of 8 *tfap2a*$^{-}$/*c*^{MO} embryos). **K, L** Dorsal and **M, N**, lateral views of 28 hpf embryos processed to reveal *foxd3* expression, which labels **K**, satellite cells (arrowheads) and **M**, Schwann cells associated with lateral line processes (arrowheads) in a control embryo, but not in **L**, **N**, a *tfap2a*$^{-}$/*c*^{MO} embryo (12 of 12 *tfap2a*$^{-}$/*c*^{MO} embryos). **O**, **P** Lateral views of 28 hpf embryos processed to reveal *eya1* expression, which is detected in the migrating lateral line migrating primordium (llmp) in **O**, a control embryo, but absent in **P**, a *tfap2a*$^{-}$/*c*^{MO} embryo (11 of 11 *tfap2a*$^{-}$/*c*^{MO} MO embryos). *eya1* expression in presumed pectoral fin mesoderm (pfm) remains normal in the *tfap2a*$^{-}$/*c*^{MO} MO embryo (11 of 11 *tfap2a*$^{-}$/*c*^{MO} MO embryos). **Q, R** Lateral head views of 4 dpf embryos incubated in DASPEI, which is taken up by hair cells. In **Q**, a control embryo, DASPEI-positive hair cells in the inner ear (arrowhead) and the neuromasts (arrows) are visible. In **R**, a *tfap2a*$^{-}$/*c*^{MO} embryo, DASPEI positive cells are not seen. **S, T** Dorsal anterior views of 28 hpf embryos processed to reveal *eya1* expression. *eya1* expression in olfactory placode is apparent in **S**, a control embryo. In **R**, a *tfap2a*$^{-}$/*c*^{MO} embryo, a small cluster of *eya1*-expressing cells is present in this position (11 of 11 *tfap2a*$^{-}$/*c*^{MO} embryos). gV, trigeminal

ganglion; allg, anterior lateral line ganglion; ac, acoustic ganglion; pllg, posterior lateral line ganglion; gAD, anterodorsal lateral line ganglion; gAV, anteroventral lateral line ganglion; gVII, facial sensory ganglion; gIX, glossopharyngeal ganglion; gX, vagus ganglion; e, eye; ot, otic vesicle. Scale bars: **A**–**R**, 100 microns; **S**, **T**, 50 microns.

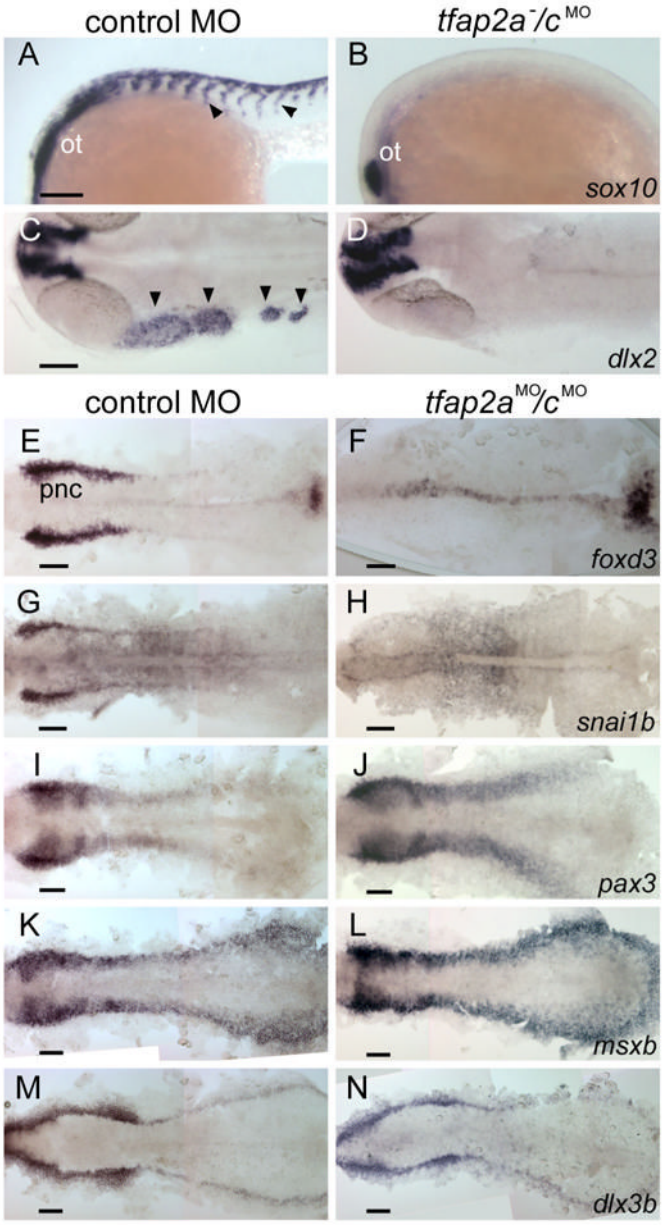

Figure 5.

Gene expression characteristic of neural crest is absent, but of the neural plate border and pre-placodal region is present in *tfap2a/c* deficient embryos. **A, B** Lateral views of 22 hpf embryos processed to reveal *sox10* expression, which is present in migratory neural crest streams (arrowheads) and the otic vesicle (ot) in **A**, a control embryo; in **B**, a *tfap2a*$^{-}$/*c*^{MO} embryo, it is only present in the ot (11 of 11 *tfap2a*$^{-}$/*c*^{MO} embryos). **C, D** Dorsal views of 24 hpf embryos processed to reveal *dlx2* expression, which is present in cranial migratory neural crest streams (arrowheads) and brain in **C**, a control embryo, but only in the latter in **D**, a *tfap2a/c* deficient embryo (10 of 10 *tfap2a*$^{-}$/*c*^{MO} embryos). **E–N** Dorsal views of flat-mounted, 11 hpf embryos processed to reveal the indicated markers. *foxd3* and *snai1b* expression that are characteristic of premigratory neural crest (pnc) cells are absent in embryos injected with *tfap2a e2i2* MO and *tfap2c e3i3* MO (hereafter, *tfap2a*^{MO}/*c*^{MO} embryo) (*foxd3*, 27 of 27 *tfap2a*^{MO}/*c* ^{MO} embryos; *snai1b*, 29 of 29 *tfap2a*^{MO}/*c*^{MO} embryos. Also not shown, at the same stage,

sox10, 29 of 29 *tfap2a*^{MO}/*c*^{MO} embryos). Expression of *pax3*, *msxb* and *dlx3b* expression appear normal in *tfap2a*^{MO}/*c*^{MO} embryos (100%, n is greater or equal to 30 *tfap2a*^{MO}/*c*^{MO} embryos for each gene, also not shown, *zic2b*). Scale bars: 100 microns.

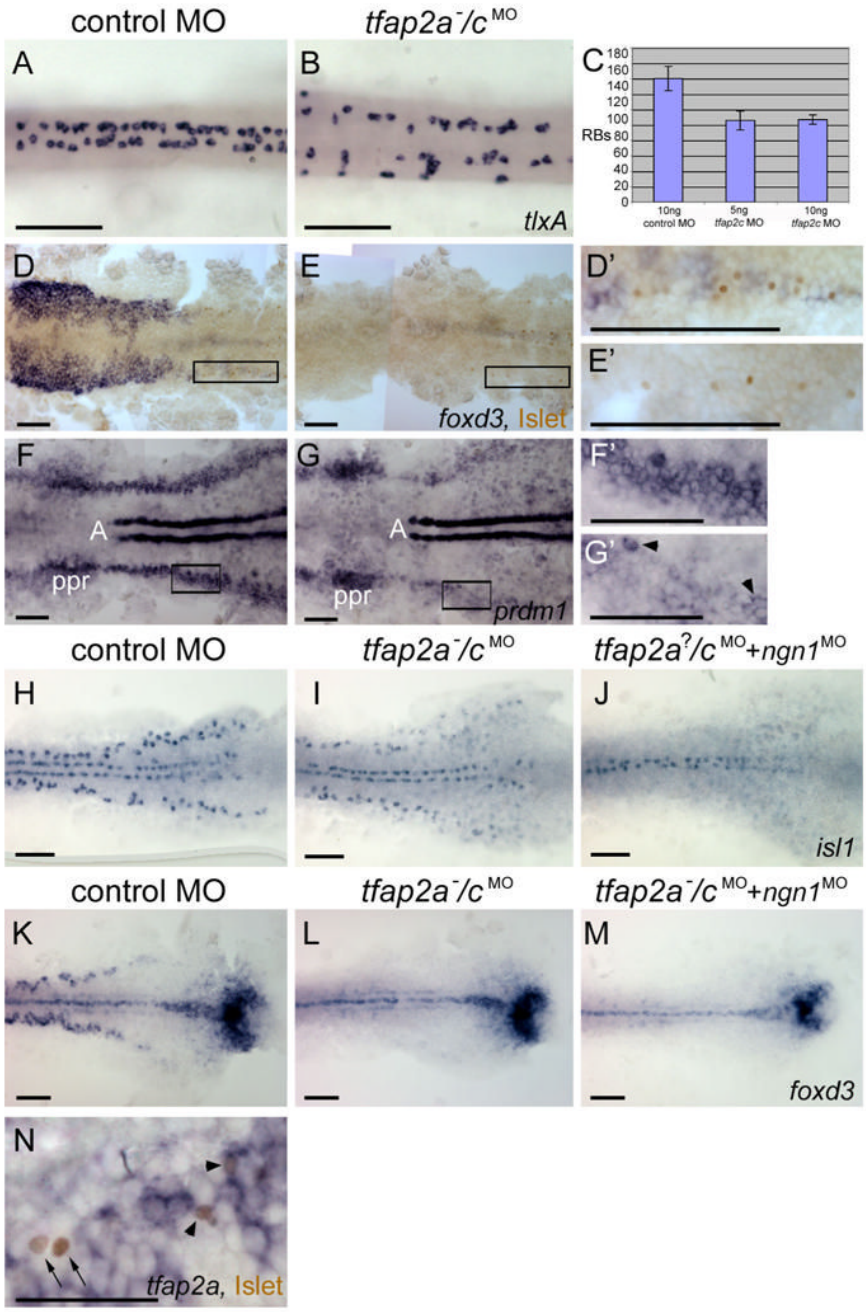

Figure 6.

Rohon-Beard sensory neurons (RBs) are reduced but not absent in *tfap2a/c* deficient embryos. **A, B** Dorsal trunk views of 20 hpf embryos processed to reveal *tlxA* expression, anterior to the left. RBs are abundant in **A**, a wild-type or *tfap2a* mutant embryo, but moderately reduced in **B**, a *tfap2a*$^{-}$/c^{MO} embryo. Note that RBs are abnormally distributed in the latter, suggestive of abnormal patterning in the dorsal neural tube. **C** The average number of *tlxA*-positive cells in the dorsal spinal cord at 20 hpf. Error bars indicate standard deviation. Left column, embryos derived from *tfap2a* heterozygous mutants and injected with control MO, n = 23 embryos. Middle column, *tfap2a* mutants injected with 5 ng *tfap2c e3i3* MO, n = 5 embryos. Right column, *tfap2a* mutants injected with 10 ng *tfap2c e3i3* MO, n = 8 embryos. **D, E** Dorsal views

of flat mounted 12 hpf embryos stained for anti-Islet immunoreactivity (brown, nuclear) and *foxd3* mRNA (purple, cytoplasmic), anterior to the left. Premigratory neural crest (pnc) cells expressing *foxd3* and RBs expressing antiIslet IR are present in **D**, a control embryo. RBs and pnc cells are intermingled, as seen at higher magnification in **D′** (corresponds to box in **D**). In **E**, a presumed *tfap2a*$^{-}$/*c*^{MO} embryo, *foxd3* expression is absent while RBs are still present, as shown at higher magnification in **E′** (11 of 40 injected embryos derived from *tfap2a* heterozygous mutants). **F**, **G** Dorsal views of flat mounted 11 hpf embryos processed to reveal *prdm1* expression, anterior to the left. In **F**, a control embryo, *prdm1* expression is detected in the pre-placodal region (ppr), in the neural plate boundary in the trunk (**F′** corresponds to box in F), and in adxial cells (A). **G**, In a presumed *tfap2a*$^{-}$/*c*^{MO} embryo, *prdm1* is expressed in scattered cells at the neural plate border (arrowheads) (**G′** corresponds to box in **G**) (7 of 29 injected embryos derived from *tfap2a*^{low} heterozygotes). **H–M** Dorsal trunk views of flat mounted 12.5 hpf embryos. *isl1* (**H**) and *foxd3* (**K**) expression shown in control embryos. **I**, In the presumed *tfap2a*$^{-}$/*c*^{MO} embryos, *isl1* expression is moderately reduced (16 of 56 injected embryos derived from *tfap2a*^{low} heterozygotes), while *foxd3* expression is absent (**L**, 12 of 58 injected embryos derived from *tfap2a*^{low} heterozygotes). **J** In an embryo derived from *tfap2a* heterozygous mutant parents and co-injected with *tfap2c e3i3* MO and *ngn1* MO, *isl1* expression in lateral neural plate, indicating RBs, is absent (48 of 51 *tfap2c* MO and *ngn1* MO injected embryos). **M** In a presumed *tfap2a* mutant injected with *tfap2c* MO and *ngn1* MO, *foxd3* expression is absent (**M**, 16 of 53 injected embryos derived from *tfap2a*^{low} heterozygotes). **N** Dorsal view of a 12.5 hpf embryo processed to reveal anti-Islet IR (brown, nuclear) and *tfap2a* mRNA (purple, cytoplasmic), anterior to the left. Some RBs that are positive for anti-Islet IR also express *tfap2a* (arrowheads). There are also RBs that are devoid of *tfap2a* expression in the cytoplasm (arrows). Scale bars: **AM**, 100 microns; **N**, 50 microns.

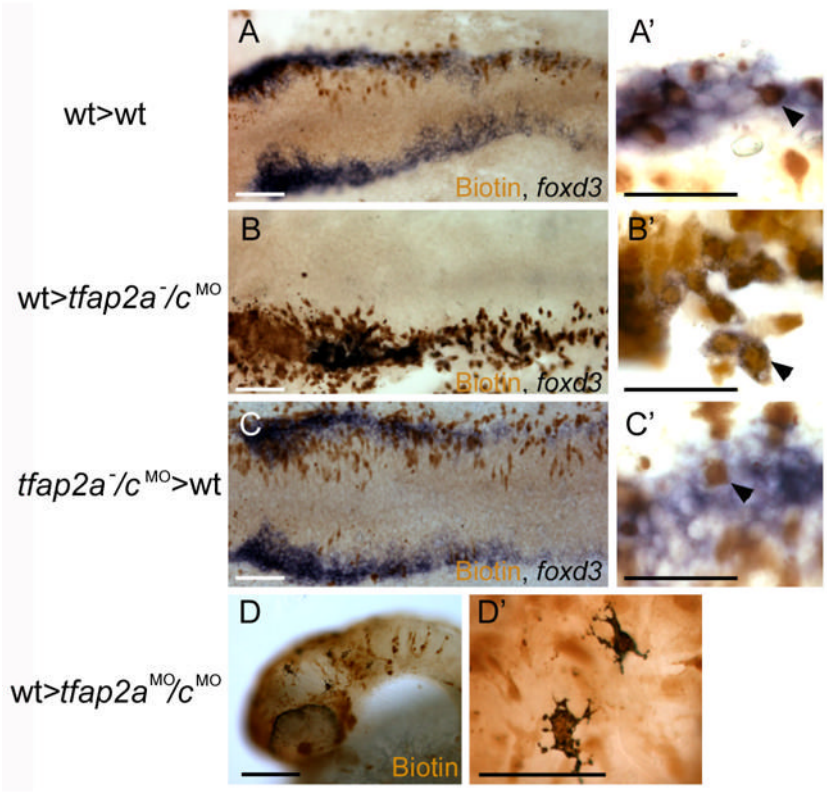

Figure 7.

Chimera experiments suggest requirement for Tfap2a/c activity in neural crest induction is cell autonomous. **A**–**C** Dorsal views of flat mounted 12 hpf embryos. **A** A chimera derived from a wild-type host and a wild-type donor. Biotin-labeled, donor derived cells are seen to express *foxd3* (arrowhead in **A′**) (a total of 40 biotin-labeled *foxd3*-expressing cells were found, 3 embryos scored). **B** A chimera derived from a *tfap2a*$^{-}$/*c*^{MO} host and a wild-type donor. Biotin-labeled, donor derived cells expressing *foxd3* are visible (arrowhead in **B′**) (150 of 151 *foxd3*-expressing cells were also biotin-labeled, 5 embryos scored). **C** A chimera derived from a wild-type host and a *tfap2a*$^{-}$/*c*^{MO} donor embryo. A biotin-labeled, *foxd3* negative cell is seen interspersed with host cells expressing *foxd3* (shown at higher magnification in **C′**, arrowhead) (of 95 biotin-labeled cells within the host *foxd3* domain, none expressed *foxd3*, 6 embryos scored). **D** Lateral view of a 48 hpf a chimera derived from a *tfap2a*^{MO}/*c*^{MO} host and a wild-type donor. Melanophores are visible in the head. As seen at higher magnification in **D′**, melanophores are labeled with biotin, indicating that they are donor-derived (Out of 30 such chimeras that survived to 48 hpf, 11 had at least 5 or more biotin-positive melanophores and lacked melanophores without biotin). Scale bars: **A**, **B**, **C**, **D**, 100 microns; **A′**, **B′**, **C′**, **D′**, 50 microns.

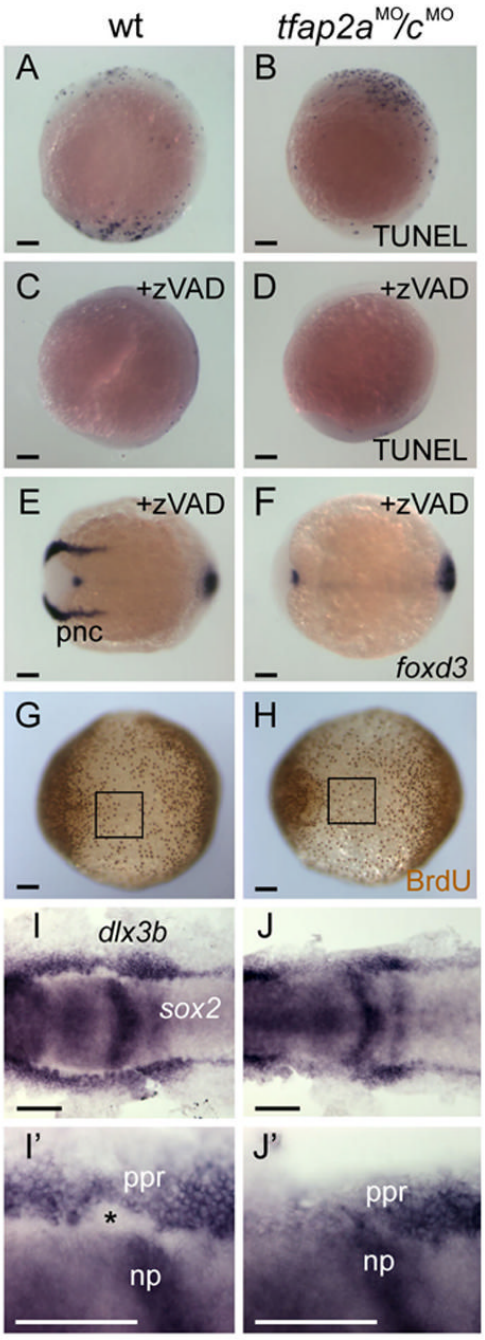

Figure 8.

Loss of neural crest in *tfap2a/c* deficient embryos is concomitant with an expansion of neural plate. **A–D** Lateral views, dorsal to the right, of either uninjected wild type or *tfap2a*^{MO}/*c*^{MO} embryos fixed at 11hpf and processed to reveal dying cells with TUNEL. A wild-type embryo and a *tfap2a*^{MO}/*c*^{MO} embryo have comparable numbers of TUNEL-positive cells [control embryos, 62 ± 70 (average ± standard deviation), n = 13; *tfap2a*^{MO}/*c*^{MO} embryos, 42 ± 38, n = 28; unpaired t test, p = 0.23]. **C** A wild-type embryo, and **D**, a *tfap2a*^{MO}/*c*^{MO} embryo, after treatment with caspase inhibitor zVAD-fmk. Reduced levels of cell death are seen in both of them (control embryos, 10 ± 14, n = 19, $p < 0.005$ in comparison to untreated controls; *tfap2a*^{MO}/*c*^{MO} embryos, 17 ± 13, n = 18, $p < 0.05$, in comparison to untreated *tfap2a*^{MO}/

c^{MO} embryos). Dorsal views, anterior to the left, of **E**, a wild-type embryo, and **F**, a *tfap2a*^{MO}/c^{MO} embryo treated with zVAD-fmk and processed to reveal *foxd3* expression at 11 hpf. *foxd3* expression is absent in the premigratory neural crest (pnc) domain of the zVAD treated *tfap2a*^{MO}/c^{MO} embryo (30 of 30 zVAD treated *tfap2a*^{MO}/c^{MO} embryos). **G, H** Ventral views, anterior to the left, of embryos incubated in BrdU for 20 minutes at 10 hpf, fixed at 11 hpf, and stained for anti-BrdU IR. The number of anti-BrdU IR positive cells within a 200x200 μm region of ventral ectoderm (boxes in G and H) was comparable in both groups (control embryos, 37 ± 6 anti-BrdU IR positive cells, n = 9 embryos; *tfap2a*^{MO}/c^{MO} embryos, 35 ± 7 anti-BrdU IR positive cells, n = 9 embryos; unpaired t test, p = 0.48). **I, J** Dorsal views of 11 hpf embryos processed to reveal *sox2* expression, labeling neural plate (np), and *dlx3b* expression, labeling the pre-placodal region (ppr). **I′, J′** Close-up views of right side of embryos shown in **I** and **J**, respectively. The space between these two expression domains, normally occupied by premigratory neural crest (asterisk in **I′**), is absent in the *tfap2a*^{MO}/c^{MO} embryo (**J**, 30 of 32 *tfap2a*^{MO}/c^{MO} embryos). Scale bars: **A–J**, 100 microns; **I′**, **J′**, 50 microns.

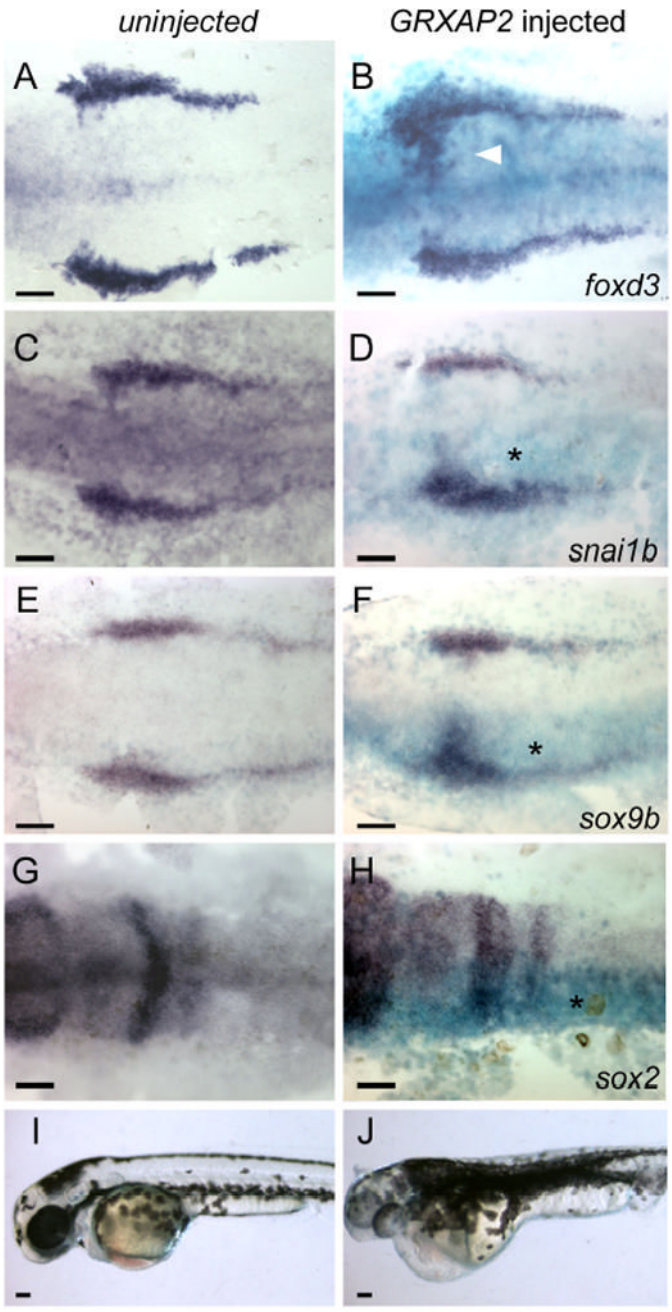

Figure 9.

Misexpression of *Xenopus TFAP2A* expands neural crest into the neural plates. **A**, **C**, **E**, **G**, **I** Uninjected control embryos or **B, D, F, H, J** embryos co-injected with RNA encoding β–galactosidase and GRXAP2, treated with dexamethasone at 8 hpf. **AH** Embryos fixed at 11 hpf, and processed to reveal β-galactosidase activity (turquoise) (**B, D, F, H**) and expression of the indicated gene (dark blue). Expression of neural crest markers is seen to be expanded into the rostral domain of the neural plate on the injected side of the embryo (asterisk) (*foxd3*, 29 of 37 embryos; *snai1b*, 31 of 40 embryos; *sox9b*, 34 of 45 embryos) while expression of neural plate marker *sox2* is decreased on the injected side (37 of 50 embryos). **I**, **J** Lateral

views of live embryos at 36 hpf, showing a massive expansion of melanophores in the *GRXAP2*-injected embryo (27 of 34 RNA-injected embryos). Scale bars: 100 microns.

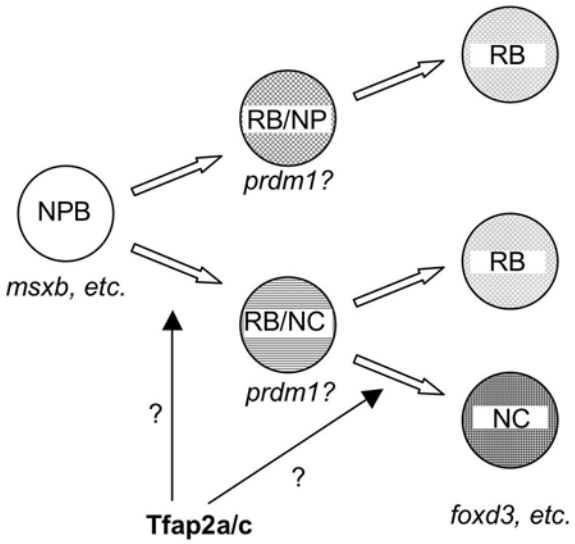

Figure 10.

Model for the role of Tfap2a/c activity in specification of trunk neural crest and RBs. At cranial levels, Tfap2a and Tfap2c, acting redundantly in neural plate border precursor (NPB) cells and in concert with other transcription factors expressed in these cells (Msx, Pax, and Zic family members), specify neural crest. At trunk levels, Tfap2a/c activity specifies RB/neural crest (NC) precursor cells, which may be identified by expression of *prdm1*. In *tfap2a/c* deficient embryos, RB/NC precursors are lost, resulting in the loss of NC, which is characterized by expression of *foxd3*, *snai1b*, *sox10*, and other genes, and a subset of RBs. The RBs that remain in *tfap2a/c* deficient embryos derive from a hypothetical precursor cell with potential to become RB and other unidentified neural plate (NP) cells (i.e., the RB/NP precursor). The RB/NP precursor cell may also be characterized by *prdm1* expression. Alternatively in the trunk, Tfap2a/c activity governs specification of NC from RB/NC precursors, in which case all RBs may derive from RB/NC precursors.